Is wear-particle induced osteolysis affecting bone formation? Does adenosine A_{2A} receptors activation modify it?

By
Tamara Zmölnig

Practical Training Semester at the NYU Langone Medical Center
Area of emphasis/ field of specialty: Molecular Biology-Orthopaedics
Degree program: Medical and Pharmaceutical Biotechnology, Bachelor
Enrolled University: IMC University of applied sciences Krems
Internal Supervisor: Dr. Christian Klein
External Supervisor: Dr. Aránzazu Mediero/Dr. Bruce Cronstein
Submitted on: 15.03.2013

Table of content

Acknowledgements

My internship at the **New York University Langone medical center** was generously funded by the **Austrian Marshall Plan foundation**. I would like to thank them for their support!

I am very thankful to our rector at the **IMC University of Applied Sciences Krems**, *Dr. Eva Werner* and our medical and pharmaceutical biotechnology team, especially *Dr. Wolfgang Schütt, Dr. Harald Hundsberger, Dr. Christian Klein, Dr. Barbara Entler and Mrs. Elisabeth Garschall,* who have all been of great help and support throughout this practical training semester.

I would also like to thank my supervisors and colleagues from the NYULMC: *Dr. Bruce Cronstein, Dr. Aranzazu Mediero, Dr. Miguel Perez Aso, Mrs. Lilly Sypher, Mrs. Tuere Wilder* and also *Dr. Partridge´*s lab team at the **NYU School of dentistry** for relocating us in their facilities after Hurricane Sandy.

Last but not least, I would like to thank my **family** and **friends** who contributed to this enriching experience.

List of figures

Abbreviations

THA	Total hip arthroplasty
$A_{2A}R$	Adenosine 2A receptor
$A_{2A}KO$	Adenosine 2A receptor knock-out
WT	Wild type
UHMWPE	Ultra high molecular weight polyethylene
Gi	Inhibitory G-protein
Gs	Stimulating G-protein
ATP	Adenosine triphosphate
cAMP	Cyclic adenosine monophosphate
ECM	Extra cellular matrix
OB	Osteoblast
OC	Osteoclast
RANK	Receptor activator nuclear factor-kappa B
RANKL	Receptor activator nuclear factor-kappa B ligand
OPG	Osteoprotegerin
IHC	Immunohistochemistry
AB	Antibody
AG	Antigen
PFA	Paraformaldehyde
dH_2O	distilled water
EDTA	Ethylenediaminetetraacetic acid
PBS	Phosphate buffered saline
BSA	Bovine serum albumin
HRP	Horseradish peroxidase
DAB	Diaminobenzidine
PFA	Paraformaldehyde
TE	Tris- EDTA buffer
H_2O_2	Hydrogen peroxide
SPARC	Secreted protein acidic and rich in cysteine
RT	Reverse transcriptase

RNA	Ribonucleic acid
cDNA	complementary DNA
DNA	Deoxyribonucleic acid
RT-PCR	Real-time polymerase chain reaction

1. Abstract

Total hip arthroplasty is subject to numerous revisions due to the degradation of the implant into wear particles causing joint inflammation and inducing osteolysis. Previous studies suggest that osteolysis is prevented by adenosine A_{2A} receptor ($A_{2A}R$) activation by $A_{2A}R$ agonist CGS21680. We explored the possibility that osteolysis affects bone formation and that $A_{2A}R$ activation modifies this. In the in-vivo studies, wear particles were applied to C57BL/6 mice calvaria and treated with saline or CGS21680 daily and locally. Bone formation was analyzed by in-vivo imaging after injecting the mice with a Xenolight probe and the calvaria were further prepared for immunohistochemistry staining to identify bone markers. In the in-vitro studies, bone marrow primary cells from mice tibia and femur were isolated, differentiated into osteoblasts and simply treated with CGS21680 or pretreated with $A_{2A}R$ antagonist, ZM241385. The differentiated osteoblasts were stained by Alizarin red staining to show the difference in calcific deposition upon sham, control and $A_{2A}R$ activated osteoblasts. The expression of receptor activator nuclear factor-kappa B ligand and osteoprotegerin by these osteoblasts was analyzed with RT-PCR. The results from these studies suggested that bone formation was prevented by wear-particles induced osteolysis and that the $A_{2A}R$ activation with CGS21680 indirectly stimulated bone formation upon osteoclasts and osteoblast coupling.

2. Introduction

Total hip arthroplasty (THA) (as seen in figure 1) is considered to be one of the most successful and cost-effective clinical surgeries in healthcare nowadays as it improves the living conditions of patients affected by debilitating hip disease such as osteoarthritis [1]. However, this surgical procedure is complicated by implant degradation into wear particles inducing osteolysis and aseptic mechanical loosening of one or both of the components [2, 3]. These complications lead to an estimation of tens of thousands of revisions per year in the United States only [4]. Wear debris are generated in different ways and include particles from various components of the prosthesis (metal, polyethylene, or ceramic) and bone cement [5]. These wear debris can stimulate the recruitment of inflammatory-mediating cells and osteoclasts (OCs) to the local site [4]. To improve long-term patient outcomes, it is essential to understand the causes of failure and the type of procedures for THA revision [6]. The major causes of prosthesis loosening are joint inflammation and OC-mediated bone resorption in response to the wear debris near the prostheses. Bone growth onto the surface of the implant is one of the most important factors for a long term survival of joint components [7].

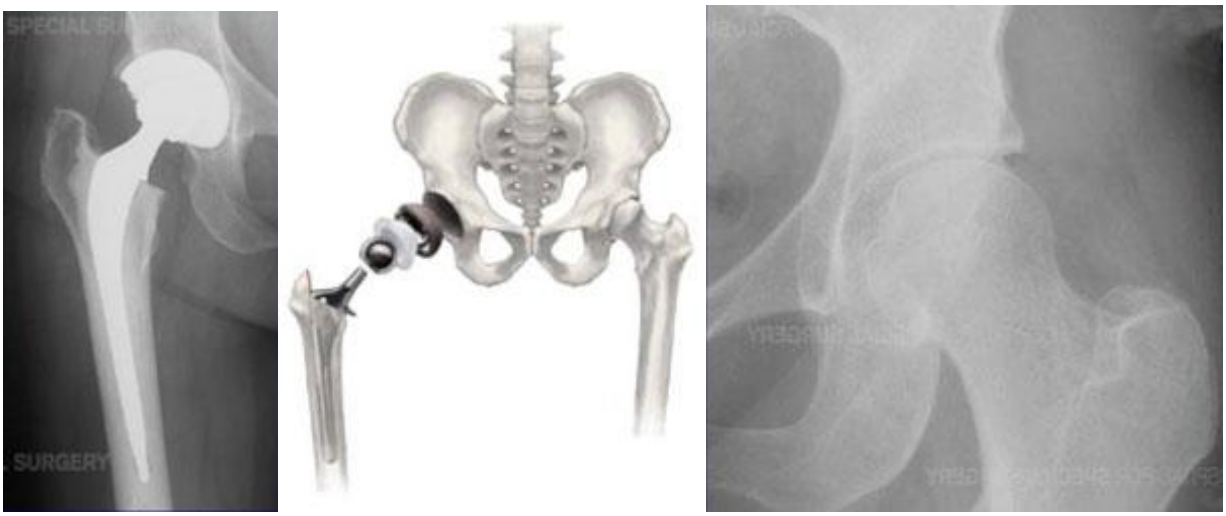

Figure 1: Comparison of a normal hip joint and total hip arthroplasty.

Taken on January 9, 2012 from http://www.hss.edu/conditions_hip-replacement-for-arthritis-of-hip.asp

2.1. Bone metabolism

Bones are specialized connective tissues covering different functions such as locomotion, protection of the internal organs and bone marrow. They are the source of metabolic storage in our bodies [8]. Bones consist of different type of cells and the extracellular matrix (ECM). The ECM is composed mostly of type I Collagen fibers and several non-collagenous proteins such as receptor activator nuclear factor-kappa B ligand (RANKL) or osteoprotegerin (OPG). These proteins have intrinsic and also metabolic functions. Bone remodeling is a dynamic process with a regulated coupling between osteoblasts (OBs) that ensure bone formation and OCs that ensure bone resorption to maintain bone integrity and homeostasis [8-10]. OBs are bone forming mononucleated cells derived from specialized mesenchymal stem cells (MSC) from the influence of specific signals that have undergone differentiation to become mature. These MSCs also form chondrocytes, myocytes and adipocytes. OBs are cuboid-shaped and cover bones by forming clusters on the bone surface. They synthesize and excrete the collagenous and non-collagenous bone matrix proteins deposited between the OBs and bone surface, they are metabolically highly active. OCs are multinucleated cells derived from hematopoietic monocytic precursor cells. They are responsible for bone resorption and degradation by demineralizing inorganic bone components and then removing the organic bone matrix [9]. Bone remodeling envelops the development of bone growth, post developmental maintenance and repair of bone and calcium provision. The coupling is regulated at 3 levels: direct interaction between OBs and OCs, local interactions and neuroendocrine systemic control of bone metabolism [8].

An important local interaction regulating the coupling between OC and OB occurs when RANKL, secreted by OBs and expressed on the surface of these cells, links to its receptor through receptor activator nuclear factor-kappa B (RANK) on the surface of pre-OCs. The binding of RANKL to RANK stimulates OC differentiation. When OBs secrete OPG, this soluble decoy receptor blocks RANK/RANKL interaction by binding to RANKL and prevents OCs differentiation and activation [9] (as seen in figure 2). The OPG-RANKL ratio is important. When less OPG is secreted by the OBs, more RANKL is secreted in the osteolysis model to maintain bone homeostasis.

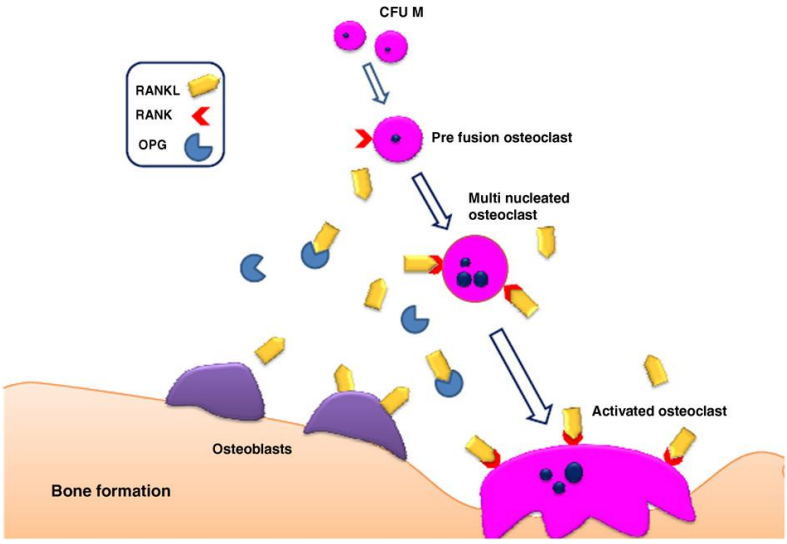

Figure 2: RANK/RANKL/OPG pathway of osteoclastogenesis.

From the article: Armelle Dufresne A. et al., Giant-cell tumor of bone, anti-RANKL therapy. BoneKEy Reports, 1; 149 (2012)

Coupling between OC and OB involve the secretion of RANKL and OPG from the OBs. When RANKL binds to RANK, OCs differentiate. When OPG, decoy protein of RANKL, binds to RANKL, it inactivates RANKL´s ability to bind to RANK, leading to the inhibition of OC differentiation.

2.2. Adenosine A_{2A} receptor

Adenosine is generated from adenine nucleotides catabolism in response to oxidative stress, ischemia and hypoxia. It is known to be involved in different metabolic pathways [11]. It is the metabolic product of adenine nucleotide dephosphorylation generated intra and extracellularly. So far, four subtypes of adenosine receptors have been discovered: A_1, A_{2A}, A_{2B} and A_3 (as seen in figure 3). Each encodes different genes and different pharmacological functions. Each of these adenosine receptor subtypes have adenosine as an agonist and its intracellular concentration is never zero [12]. They are all are G-protein coupled receptors [12]. The A_{2A} and A_{2B} receptors interact with G_s family G proteins stimulating adenylyl cyclase. A_1 and A_3 interact with $G_{i/o}$ proteins and other G proteins [13]. The G_i inhibits adenylyl cyclase. When adenosine binds to the A_{2A} G-protein coupled receptor, the $A_{2A}R$ is coupled to the G_s protein. The α-subunit of the Gs protein is detached from the ß and λ dimer subunit complex. This leads to the activation of the α-subunit, activating the adenylate cyclase signaling pathway. ATP is converted

to cAMP, which operates as a second messenger. This second messenger bifurcates the signal to phospholipase C pathway, PKA and EPAC.

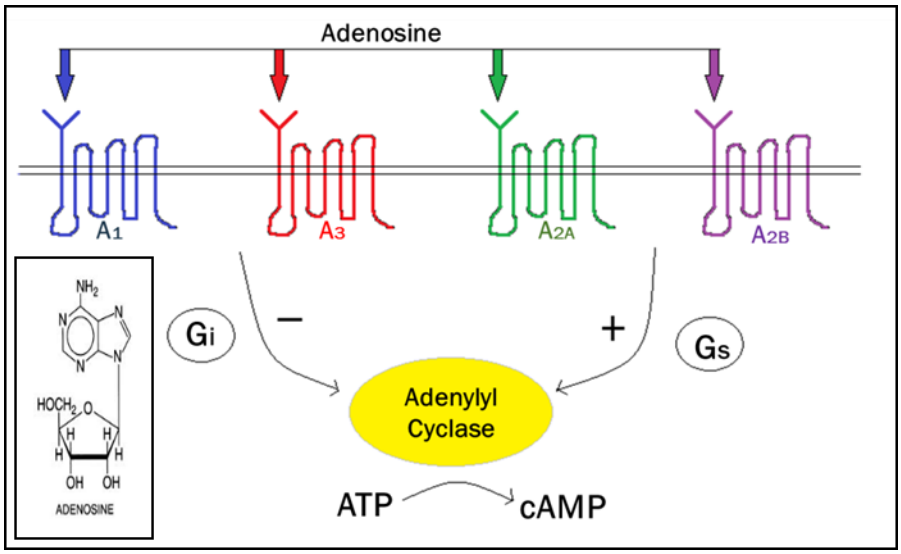

Figure 3: The four subtypes of adenosine receptors

A_1 and A_3 receptors activate Gi which inhibits adenylyl cyclase. A_{2a} and A_{2B} receptors activate Gs which stimulates adenylyl cyclase converting ATP into cAMP.

Results from previous studies on OCs demonstrated that $A_{2A}R$ had the ability to prevent wear particle-induced osteolysis and OC formation in-vitro and in-vivo and therefore prevent joint inflammation caused by implant degradation induced wear particles called UHMWPE (ultrahigh molecular weight polyethylene particles) (as seen in figure 4). In the in-vitro studies, OCs differentiation was prevented in presence of $A_{2A}R$ agonist, CGS21680, and pretreatment with the $A_{2A}R$ antagonist, ZM241385, reverted this effect as pretreatment with ZM241385 blocks CGS21680 from binding to the $A_{2A}R$, therefore disabling the $A_{2A}R$ activation. Both in vitro and in vivo experiments demonstrated that the inhibitory effect of the $A_{2A}R$ was effective because there was no bone resorption inhibition in the $A_{2A}KO$ mice. This shows the specific role of $A_{2A}R$ in OC differentiation inhibition. These findings could lead to the improvement of hip implants by reducing inflammation and bone resorption, caused by the hip implant induced wear particles [4, 14].

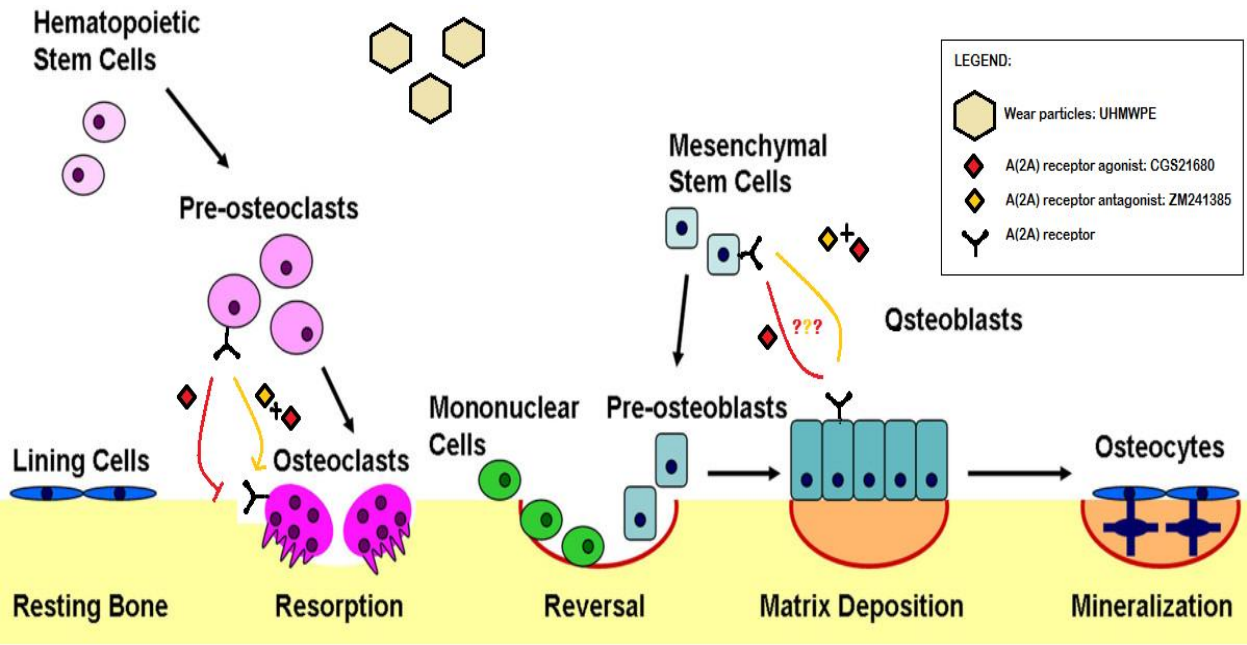

Figure 4: Bone remodeling in presence of wear particles causing osteolysis.

Modified review image from Kapinas, K. and Delany, A. MicroRNA biogenesis and regulation of bone remodeling, Arthritis Research & Therapy 13:220 (2011)

OCs resorb bone mineral and matrix. Mononuclear cells prepare the resorbed surface for OBs, which generate newly synthesized matrix as they differentiate. Matrix mineralization and the differentiation of some OBs into osteocytes completes the remodeling cycle. The A (2A) R agonist prevents osteolysis from wear particles and A (2A) receptor antagonist stimulates it. The role of the A (2A) R on bone formation will be determined in this project by treating OBs with A (2A) R agonist and antagonist in an osteolysis model.

The following project determines if wear particles-induced osteolysis affects bone formation and if $A_{2A}R$ activation modify it (as seen in figure 4).

3. Materials and methods

3.1. In vivo studies

3.1.1. Wear particles preparation

UHMWPE particles were a gift from P.H Wooley via Christi Regional medical center with particle size average of 1.74 ±1.43 µm. They were decontaminated by washing twice with 70% Ethanol for 24 hours at room temperature. The particles were washed with PBS and dried in a dessicator.

3.1.2. Surgical procedure: incision and wear particles application

After anesthesizing 15 C57BL/6 wild type (WT) male mice by intraperitoneal injection of ketamine (100 mg/kg) and xylazine (10 mg/kg), a 1-cm incision was made on the calvaria scrapped with a scalpel. The mice were separated into three groups. The sham group (n=5) had an incision closure with calvaria scrapping, no wear particle application and no treatment. The others received 3 mg of dried UHMWPE particles at the site of incision and the calvaria were scrapped: the control group (n=5) was injected with 20 µl of saline at the site of incision and the $A_{2A}R$ agonist treated group (n=5) received 20 µl of 10^{-6}M CGS21680. The mice were locally injected daily with their corresponding treatments until sacrifice at day 14 post-surgery. Bone formation was analyzed on day 8 by in-vivo imaging IVIS using Xenolight rediject bone probe 680 injected on day 7 post-surgery. After euthanizing the mice on day 14, the calvaria were collected and prepared for IHC (as seen in figure 5).

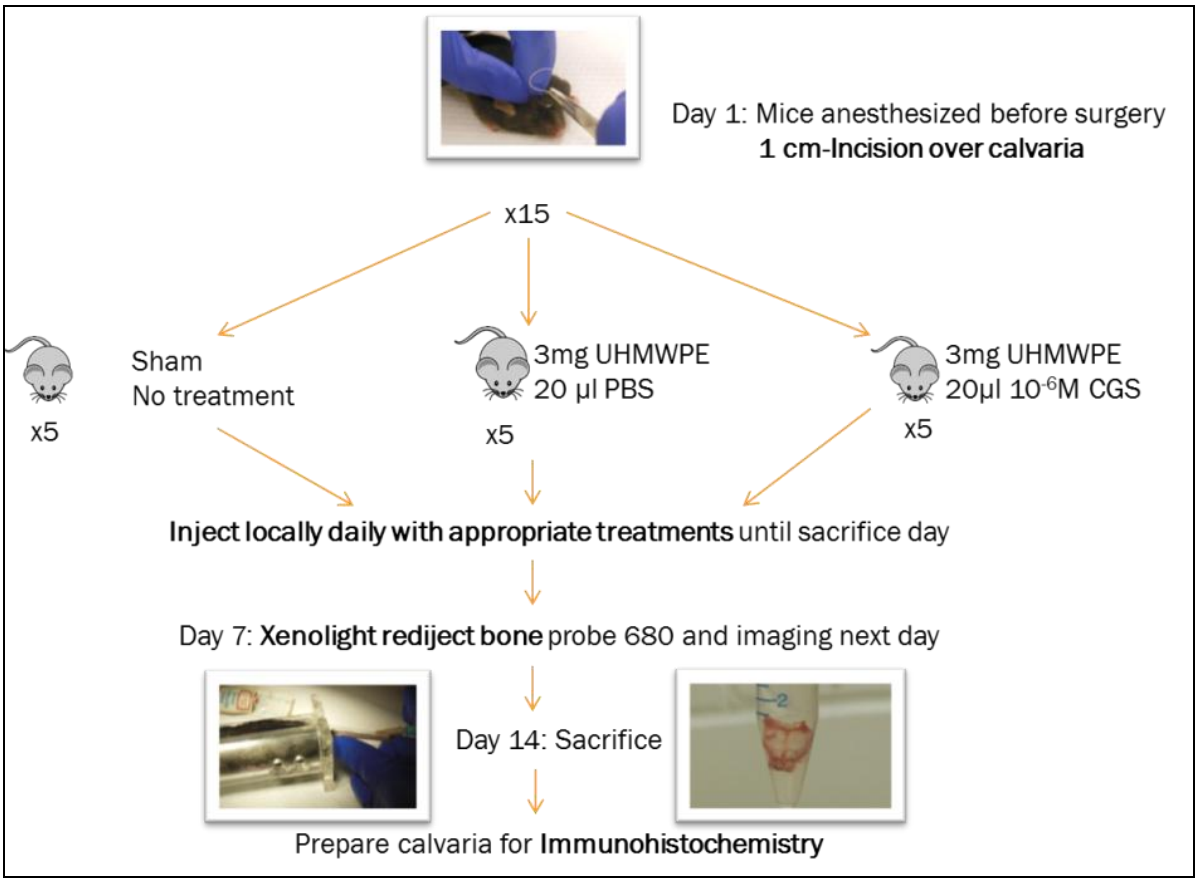

Figure 5: Planning of the in-vivo studies from incision to sacrifice

The C57BL/6 WT mice were maintained on C57BL/6 background by the breeder from Taconic laboratories. A_2AKO mice were a gift of J. F. Chen (Boston University School of Medicine).

Notice: The IHC slides preparation from the mice calvaria in this experiment were delayed due to Hurricane Sandy. This same experiment was done previously with WT and A_2AKO mice by practical training external supervisor, Dr. Aranzazu Mediero. Some of the IHC slides from these previous A_2AKO mice were used to examine the specificity of the A_{2A} receptor agonist, CGS21680. A dose response with CGS21680 was done with the previous WT mice.

3.1.3. Xenolight injection and imaging

On day 7, the mice were anesthetized by isoflurane inhalation and positioned in a restrainer. 150 µl of Xenolight rediject probe was injected laterally into the tail vein of the mice with a sterile syringe and the tail was swabbed with ethanol after injection. The hair over the calvaria area was removed with an electric razor and Nair®. The anesthetized mice were placed in the IVIS® Spectrum for live imaging of bone formation on the mice calvaria.

3.1.4. Histological studies: Immunohistochemistry (IHC) with seven different bone formation and resorption markers

After collecting the calvaria from the sacrificed mice, the calvaria were fixed in 4% PFA. 48 hours later, the calvaria were decalcified in 10% EDTA and changed daily for 4 weeks. The calvaria were then washed with dH_2O for 3 hours. They were incubated in 70% ethanol overnight. The following day, the calvaria were incubated in 80% ethanol for 2 hours, in 90% ethanol for 2 hours and in 100% ethanol overnight. The next day, the calvaria were incubated in 100% ethanol for one hour. They were than incubated in 100% ethanol and given to a specialized technician. This technician embedded the calvaria in paraffin and sectioned the calvaria embedded paraffin blocks with a thickness of 5 µm and affixed the samples on slides.

The sectioned calvaria embedded in paraffin were pre-deparaffinized by heating the slides in 60°C for 30 minutes. The deparaffinization step was done by immersing the slides in 3 washes for 10 minutes in Xylene. The sections were rehydrated by immersing the slides in graded washes of ethanol: 100% ethanol for 2 minutes, 90% ethanol for 2 minutes, 80% ethanol for 2 minutes, and 70% ethanol for 2 minutes. A final wash in dH_2O for 5 minutes is done to fully rehydrate the sections. The antigen (AG) retrieval method used was the proteolytic induced epitope retrieval (PIER) Proteinase K method using Proteinase K stock solution added to TE buffer.

The sections were immersed in a coplin jar with proteinase K solution (20 ug/ml in tris-EDTA buffer, ph= 8.0) for 15 minutes in waterbath at 37°C. Afterwards, the sections were rinsed 2 times for 2 minutes with PBS. The internal peroxidase removal was done with 3% H_2O_2 in methanol by sections incubation for 15 minutes at room temperature. Sections were rinsed with 3 times with 3% BSA.

The blocking is done to block the reactive sites that the primary and secondary ABs may mistake for the right binding site avoid nonspecific proteins binding that can lead to high background or false results. The blocking in this experiment was done with blocking buffer by sections incubation for 1 hour at room temperature.

The primary AB was diluted in 3% BSA in PBS (RANK (Abcam), 1:100; RANKL (Abcam), 1:200; Osteopontin (Abcam), 1:100; Osteocalcin (Abcam), 1:200; Osteoprotegerin (Abcam), (0.5 ug/ml), Alkaline phosphatase (Abcam),1:250; Type I collagen (Southern Biotech), 1:20; Osteonectin (SPARC) (Abcam), 1:100) and the slides were covered with plastic sheets to distribute equally these primary ABs. The slides were incubated overnight at 4°C in a humidified chamber. A negative control was done by replacing the primary AB with AB diluent which was in this case 3% BSA in PBS.

The following day, 3 washes of 3% BSA in PBS were done. The diluted secondary goat anti-rabbit HRP (horseradish peroxidase) AB, (HRP (Abcam), 1:200), which was a polyclonal AB, was pipetted onto each slide and the slides were covered with plastic sheets. The slides were incubated for 1 hour at room temperature.

A wash of 3% BSA in PBS was done with additional 2 washes of PBS. Developing was done by adding diaminobenzidine (DAB) (Fast 3'3', SIGMA) on the enzyme HRP used. Upon DAB addition reacting with HRP, the enzyme conjugated to the AB-AG substrate produced a brown colored precipitate where the protein was located upon DAB addition reacting with HRP.

After washing with PBS 3 times, counterstaining was done with hematoxylin for 1 min. Counterstaining was done after the AB staining to give contrast to the primary staining and allowed showing the precise cell structure.

After the slides were completely dry, they were mounted with Permount™ (Fisher Scientific) mounting medium for long-term storage or usage by stabilizing the tissue sample stain and preventing enzymatic product degradation. The slides were scanned with brightfield scanning Leica SCN400F. This scanner was only used by specialized technician and allowed scanning entire slides with one or multiple tissue sections at different high resolution magnifications. Bone formation was analyzed by counting the brown colored positive cells in a scalable manner by zooming in or out leaving a range of 1x to 80x from the scanned images of the IHC slides on the software SlidePath's Digital Image Hub accessible with a special account to analyze the scanned images.

3.2. In vitro model

Bone marrow primary cells were isolated from C57BL/6 WT mice femur and tibia in a plate with growing media and incubated at 37°C in 5% CO2. Growing media consisted of α-MEM containing 10% FBS and 1% Penicillin-streptomycin (Invitrogen, Gibco). The floating hematopoetic precursor cells were removed the following day. The MSCs, which are the OB precursors, grew with growing media until the plate was 80% confluent. At this 80% confluence, the cells were prepared into smaller plates for RT-PCR and into 24-well plates for Alizarin red staining. When these prepared OB precursors reached once again 80% confluence, they were differentiated into OBs with osteogenic differentiating media and treated with A_{2A} receptor agonist, CGS21680 or antagonist, ZM241385. Osteogenic differentiating media consisted of α-MEM containing 10% FBS, 1% Penicillin-streptomycin, 50 mM glycerolphosphate, 10 mM Dexamethasone and 50µg/ml L-ascorbic acid.

3.2.1. Alizarin Red Staining: analysis of calcific deposition by osteoblasts

Alizarin red staining was performed on the 10th day post-differentiation to determine quantatively the presence of calcific deposition by osteogenic cells upon $A_{2A}R$ agonist or antagonist treatment. The cells were treated in 24-well plates. The alizarin red staining solution was prepared by adding 2 g of Alizarin Red S in 500 ml of dH_2O (pH 4.1-4.3). The dark-brown solution was filtered and stored in the dark. After removing the media, they were washed with Dulbecco´s PBS. After aspirating the PBS, enough 4% PFA was added to cover the cell´s monolayer and incubated for 15 minutes. After washing with dH_2O, the Alizarin red staining solution was added to cover the cellular monolayer. Incubation with Alizarin Red staining solution was done at room temperature in the dark for 45 minutes. The cells were washed four times with dH_2O after the Alizarin red staining solution was aspirated. The washing dH_2O was aspirated and PBS was added. The cells were analyzed with Sigma Scan by evaluating the red color intensity of each well. Reddish undifferentiated OBs were without extracellular calcium deposits and bright orange-red mineralized OBs were with extracellular calcium deposits.

3.2.2. RANKL and OPG expression on messenger level with RT PCR

As RANKL and OPG contribute to OC differentiation activation or inhibition upon their binding to RANK, these non-collagenous OB secreted proteins are studied by RT-PCR. This allows determining if CGS21680 modifies their expression as CGS2168 inhibits OC differentiation.

The OBs were fully differentiated on the 10th day post-differentiation and reached 80% confluence when they were collected, the cell pellet was retrieved. To retrieve the cell pellet, the media was aspirated and OBs were washed with cold PBS in order to decrease metabolism of the cells. The cold PBS was aspirated and new cold PBS was added once more. The OBs were scraped and pipetted into Eppendorf tubes. The cells were centrifuged for 15 minutes at 1 400 rpm in order to obtain a cell pellet that was stored at -80°C until the RNA extraction was performed.

RNA extraction

The RNA was extracted from the cell pellet collected from the treated plates using RNeasy Mini Kit, Quiagen.

Additional information:

- *10 µl ß-Mercaptoethanol per 1 ml RLT buffer was added right before using the kit*
- *4 volumes 96-100% ethanol was added to RPE concentrated buffer before first use*
- *Worked at room temperature*
- *DNaseI stock [1500 units] dilution: DNaseI + 550 µl RNase free water*
- *All centrifugation was done at 20-25°C in standard microcentifuge.*
- *The kit was kept at room temperature for less than 9 months*

350 µl RLT buffer was added to the cell pellet and vortexed. A QUIAshredder column for homogenation was inserted to a 2 ml tube and centrifuged for 2 minutes at high speed. 350 µl of 70% ethanol was added to the tube and mixed by pipetting. The 700 µl of sample was transferred to an RNease column link to a 2 ml collector tube. The tube was centrifuged for 15 seconds at 10 000 rpm and the eluite discarded. The tube was reused and 350 µl RW1 buffer was added to the RNeasy column, the tube was centrifuged for 15 seconds at 10 000 rpm and the eluite discarded. The tube was reused and 10 µl DNaseI + 70µl RDD buffer were added and mixed by tube inversion. The tube was incubated for 15 minutes at room temperature. 350 µl RW1 buffer was added to RNeasy column and centrifuged for 15 seconds at 10 000 rpm. The eluite was discarded. The RNeasy column was transferred to a new 2 ml collector tube. 500 µl RPE buffer was added to the column and the tube was centrifuged for 15 seconds at 10 000 rpm, the eluite was discarded. The tube was centrifuged once more for 1 minute at 13 000 rpm. The columm was transferred to a 1.5 ml cap-free tube. 30-50 µl of RNase free water was pipetted into the column, the tube was centrifuged for 1 minute at 10 000 rpm. This step was repeated a second time to obtain more of the sample. The eluite was in the same tube.

RNA quantification

The step was done by using a Nanodrop spectrophotometer. After selecting the Nucleic acid option for type RNA and measures in ng/µl, a blank measurement was done by pipetting 1 µl of sterile water to the spectrophotometer´s tip. The samples measurements were continuously analyzed by pipetting 1 µl. After obtaining the blank and samples measurements with the RNA quantification values, the reverse transcriptase was done.

Reverse Transcriptase (RT)

RT master mix was prepared as followed:

Table 1: Composition of master mix for RT

	Ci	**Cf**
MgCl2	25 mM	5 mM
10x PCR buffer	10x	1x
dATP	10 mM	1 mM
dTTP	10 mM	1 mM
dGTP	10 mM	1 mM
dCTP	10 mM	1 mM
RNA inhibitors	20 U/µl	1 U/µl
Random Hexamers	50 U/µl	2.5 U/µl
Multiscribe reverse	50 U/µl	2.5 U/µl

The RT program used was:

Table 2: Applied Biosystems GeneAmp PCR Instrument Systems´Reverse Transcriptase Profile Times and Temperatures

Times and temperatures for reverse transcriptase		
15 min	5 min	5 min
42°C	99°C	5°C

RNA was stored at -80°C and the cDNA was stored at -20°C.

RT PCR

Table 3: Composition of RT-PCR master mix

	Ci	Cf
SYBR® Green QPCR Mastermix	2x	1x
Forward primer	10 µM	0.3 µM
Reverse primer	10 µM	0.3 µM
Water	-	-

After preparing the RT-PCR master mix, 5 µl of sample cDNA and 20µl of the master mix were pipetted together into PCR tubes. The samples ran in the RT-PCR instrument and program as followed:

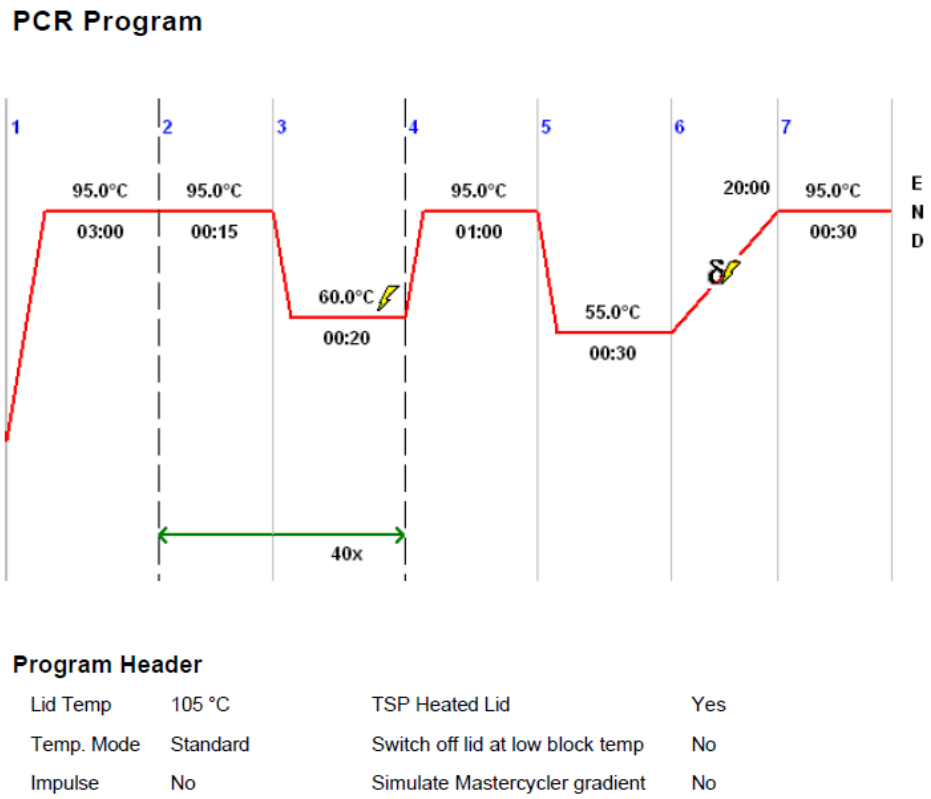

Figure 6: Snapshot from realplex 2.2 Eppendorf demonstrating the RT-PCR cycles

4. Results

4.1. In vivo study

4.1.1. Bone formation analysis with Xenolight injection

Upon Xenolight injection on the 7th day post-surgery, bone formation was analyzed via in-vivo imaging on the 8th day (as seen in figure 7). Xenolight rediject bone probe 680 is a fluorescent reagent for targeting hydroxyapatite. Hydroxyapatite, being a biomarker for OB activity is an important component of normal bone and enables the in-vivo detection, measurement and monitoring of skeletal change. The in-vivo images taken showed significant results on the effect of wear particles and the $A_{2A}R$ agonist on bone formation one day post-injection, which continued to be as significant the following days.

A

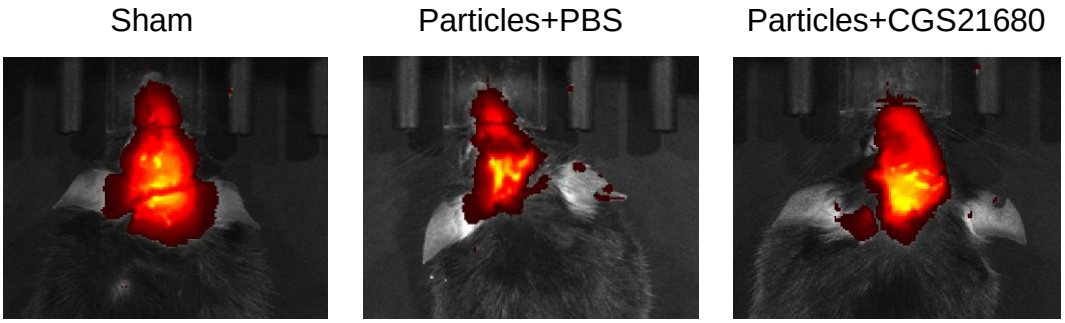

B

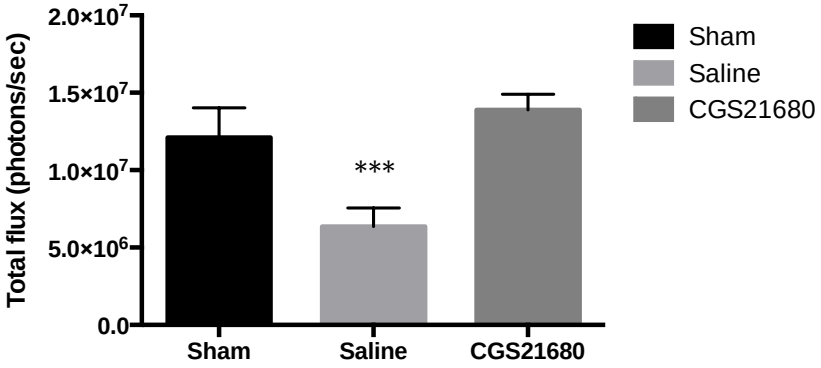

Figure 7: Xenolight injection on day 7 and imaging on day 8 post-surgery

*Day 8 after surgery: 24h after Xenolight injection (A) Images of Xenolight showing OB activity (B) Morphometric quantitation of bone formation in the presence of Saline or CGS21680 injected every day after surgery in WT mice. Data was calculated as the flux of OB activity (photon/Sec). ***P< 0.001, compared to sham, ANOVA.*

From to the Xenolight injection via the tail vein on the 7th day post-surgery, the in-vivo images taken on the 8th day showed that wear particles stimulated a decrease in new bone formation when injecting saline daily for 7 days after forming an air pouch over the calvaria of the adult male WT mice with 3mg of UHMWPE. This effect was reverted when injecting the mice locally with 10^{-6} M CGS21680.

4.1.2. Bone formation in osteolysis analysis via immunohistochemistry bone markers

Wear particles induce osteoclast-mediated bone resorption and site inflammation

After collecting the calvaria and preparing them for IHC, an H&E staining was done with the calvaria prepared in the in-vivo study of this project. The H&E staining was done by supervisor, Dr. Aranzazu Mediero.

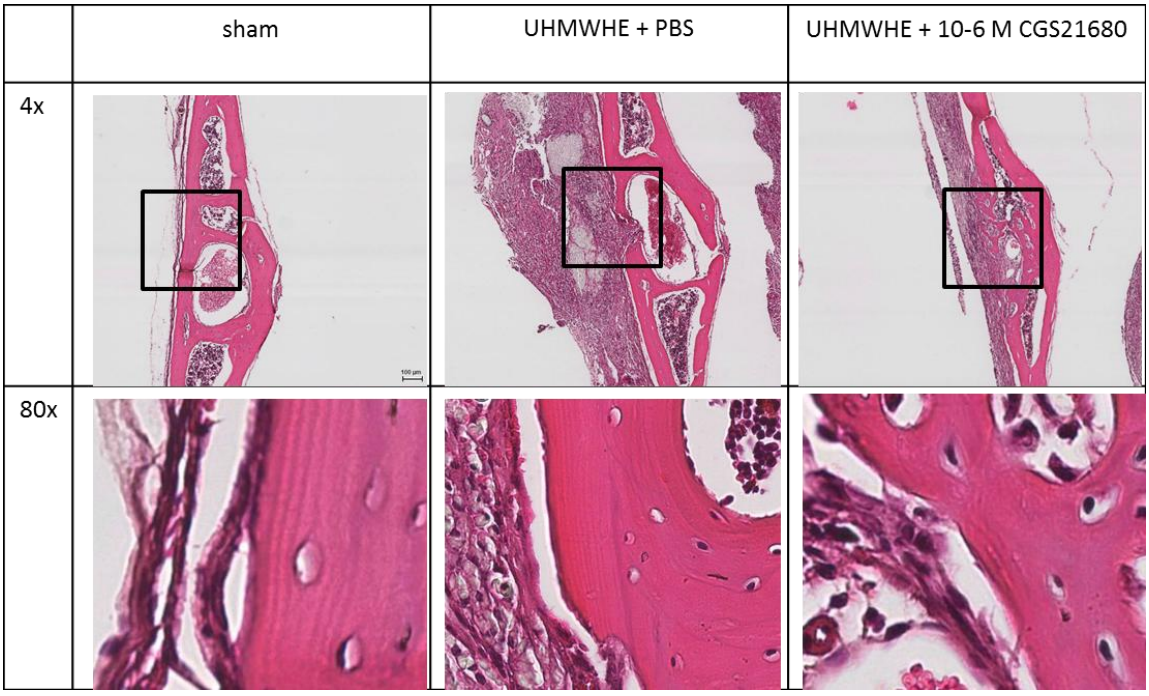

Figure 8: H&E slides showing sham mice, mice with particle insertion and saline treatment, mice particle insertion and 1µM CGS21680.

The sham calvaria shows no inflammation around the bone. The particles+ local saline treatment mice show an increase of inflammation. The particles+local 1µM CGS21680 treatment mice results are similar to sham results, there is a decrease of inflammation compared to the control mice.

These H&E results show how wear particles increased the inflammation site and bone resorption when the calvaria were injected with PBS compared to the non-treated calvaria. Treatment with the $A_{2A}R$ agonist, 1 µM CGS21680, reverted the effect of the wear particle´s ability to cause OC-mediated bone resorption and inflammation at the site of wear particles insertion. Such findings were also found in previous studies, where $A_{2A}R$ agonist prevented wear-particles induced osteolysis [4].

The examination of several immunohistochemical bone markers in treated calvaria were studied in the osteolysis model, this allowed to demonstrate the effect of wear particles on bone formation. The bone resorption and formation markers used were: Alkaline phosphatase, Osteonectin, Osteopontin, OPG, RANK, RANKL, type I collagen, Osteocalcin.

4.1.2.1. Alkaline phosphatase

A.

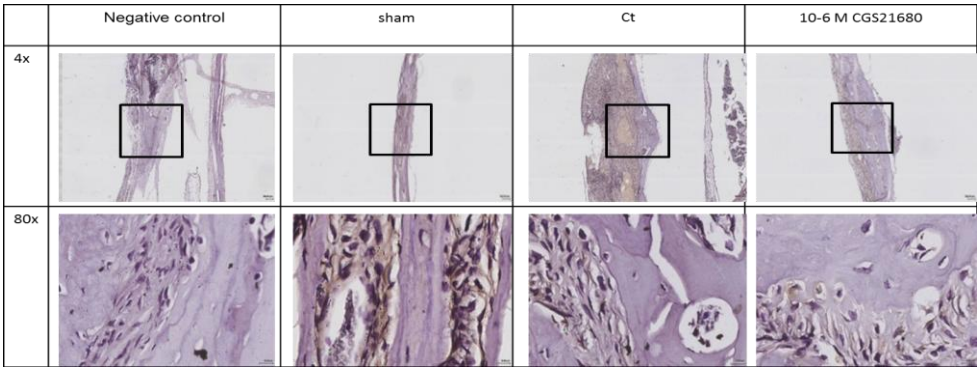

B.

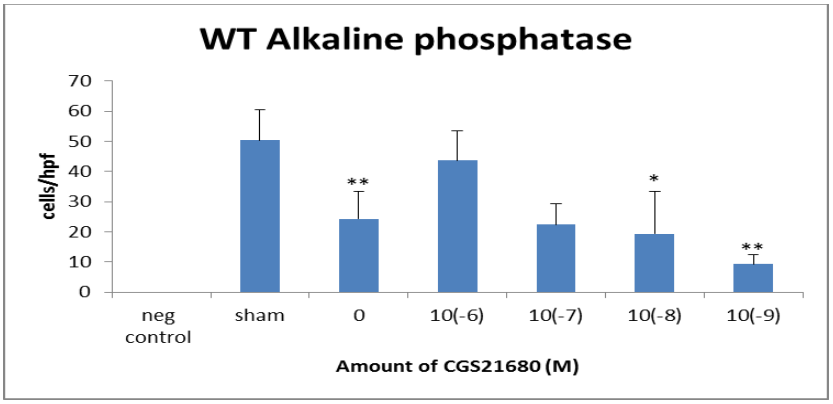

C.

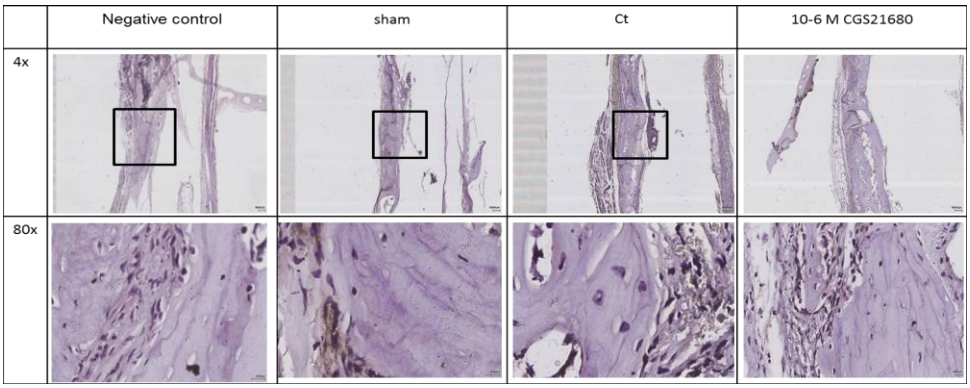

D.

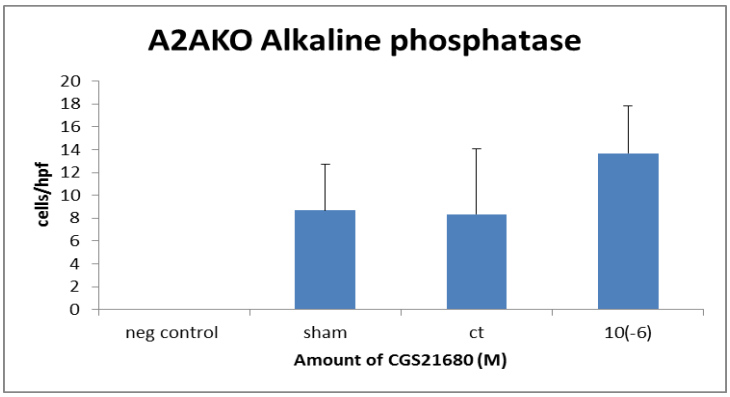

Figure 9: Immunohistochemistry for osteoblast marker: Alkaline phosphatase in WT and A_{2A}KO mice.
(**A**) Calvaria were prepared and immunohistologic staining was processed on sham or UHMWPE-exposed WT mice, treated with saline or CGS21680 (1µm). The sections shown are representative of calvaria stained for Alkaline phosphatase. All images from slides were taken at the magnifications: 4x and 80x. Scale bars100 µm for 4x and 10 µm for 80x. (**B**) Immunohistochemistry quantifications of cells/hpf for (A). Data are means ± SEM for 3 different slides per untreated mouse (n=5), and each mouse treated with particulate and saline (n=5) or particulate and 1 µm of CGS21680 (n=5). (**C**) Calvaria were prepared and immunohistologic staining was processed on sham or UHMWPE-exposed A(2A)KO mice, treated with saline or CGS21680 (1µm). The sections shown are representative of calvaria (from n=3 mice) stained for Alkaline phosphatase. All images were taken at the magnifications: 4x and 80x. Scale bars100 µm for 4x and 10 µm for 80x. (**D**) Immunohistochemistry quantifications of cells/hpf for (C). Data are means ± SEM for 3 different slides per untreated mouse (n=5), and each mouse treated with particulate and saline (n=5) or particulate and 1 µm of CGS21680 (n=5). *P<0.5;**P<0.01; ***P< 0.001, compared to sham, ANOVA.

From (figure 9 A-B), the alkaline phosphatase primary AB staining shows that the WT non-treated mice had an average of 50 ±10 positive OBs. In presence of wear particles and treatment with PBS, there was a decrease in the average of positive OBs to 24.3 ±9 (with **P<0.01) compared to WT sham. The WT mice treated with 10^{-6} M CGS21680 had an average of 43.7 ±10 positive OBs at the site of incision of UHMWPE showing an

increase compared to the WT control mice treated with PBS. In (figure 9 B), there is a dose response done with the WT $A_{2A}R$ agonist treated mice which shows the effects of the $A_{2A}R$ agonist from 10^{-6} M to 10^{-9} M, showing less positive OBs correlating to the lower concentrations of the $A_{2A}R$ agonist. In (figure 9 C-D), these $A_{2A}KO$ mice show no statistically significant difference in the number of positive OBs between the slides from the non-treated mice and the control mice or the $A_{2A}R$ agonist treated mice.

4.1.2.2. Osteonectin

A.

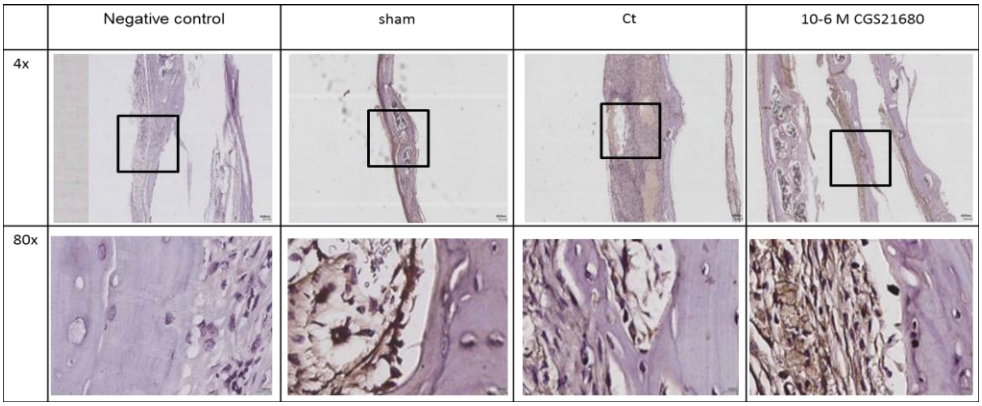

B.

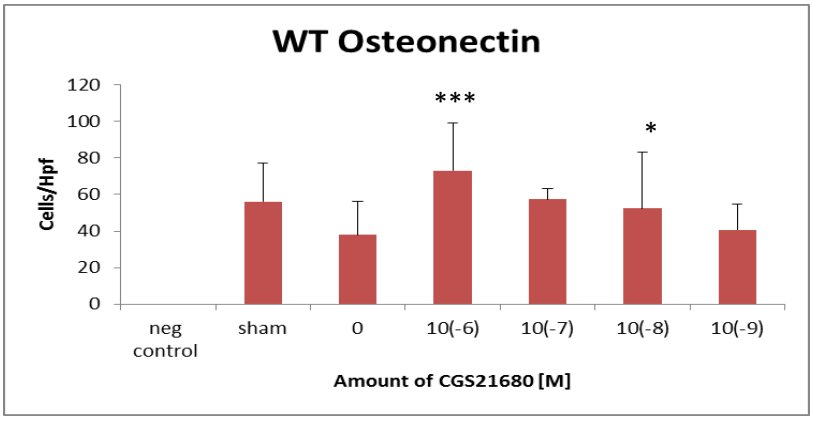

C.

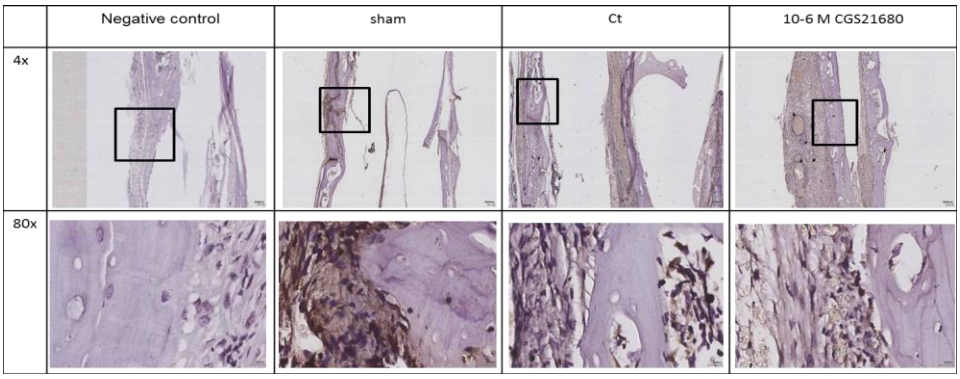

D.

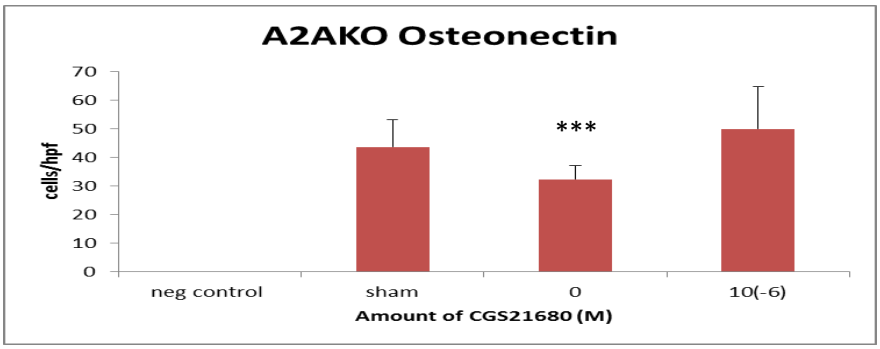

Figure 10: Immunohistochemistry for osteoblast marker: Osteonectin in WT and A_{2A}KO mice.
(**A**) Calvaria were prepared and immunohistologic staining was processed on sham or UHMWPE-exposed WT mice, treated with saline or CGS21680 (1µm). The sections shown are representative of calvaria stained for Osteonectin. All images from slides were taken at the magnifications: 4x and 80x. Scale bars100 µm for 4x and 10 µm for 80x. (**B**) Immunohistochemistry quantifications of cells/hpf for (A). Data are means ± SEM for 3 different slides per untreated mouse (n=5), and each mouse treated with particulate and saline (n=5) or particulate and 1 µm of CGS21680 (n=5). (**C**) Calvaria were prepared and immunohistologic staining was processed on sham or UHMWPE-exposed WT mice, treated with saline or CGS21680 (1um). The sections shown are representative of calvaria (from n=3 mice) stained for Osteonectin. All images were taken at the magnifications: 4x and 80x. Scale bars100 µm for 4x and 10 µm for 80x. (**D**) Immunohistochemistry quantifications of cells/hpf for (C). Data are means ± SEM for 3 different slides per untreated mouse (n=5), and each mouse treated with particulate and saline (n=5) or particulate and 1 µm of CGS21680 (n=5). *P<0.5;**P<0.01; ***P< 0.001, compared to sham, ANOVA.

From (figure 10 A-B), an osteonectin primary AB staining shows that the WT non-treated mice had an average of 56 ±21 positive OBs. For the WT mice calvaria in presence of wear particles and treatment with PBS, there was a decrease of the average of positive OBs to 38 ± 18 compared to sham. The WT mice treated with 10^{-6} M CGS21680 had an average of 73 ±26 positive OBs (***P<0.001 compared to WT sham) at the site of incision of UHMWPE showing an increase compared to the WT

control mice treated with PBS. In (figure 10 B), there is a dose response done with WT $A_{2A}R$ agonist treated mice which shows the effects of the $A_{2A}R$ agonist from 10^{-6} M to 10^{-9} M, showing less positive OBs correlating to lower concentrations of the $A_{2A}R$ agonist. In (figure 10 C-D), these $A_{2A}KO$ mice slides show a statistically significant difference in the number of positive OBs between the control mice and the non-treated mice (***P<0.001 $A_{2A}KO$ control mice compared to $A_{2A}KO$ sham), but no significant difference between the non-treated mice and the $A_{2A}R$ agonist treated mice. The number of positive OBs from the non-treated $A_{2A}KO$ mice and the $A_{2A}KO$ $A_{2A}R$ agonist treated mice were similar. This contributes to the statistical significant difference in the number of positive OBs between the $A_{2A}KO$ $A_{2A}R$ agonist treated mice and the $A_{2A}KO$ PBS treated mice when wear particles were inserted.

4.1.2.3. Type I Collagen

A.

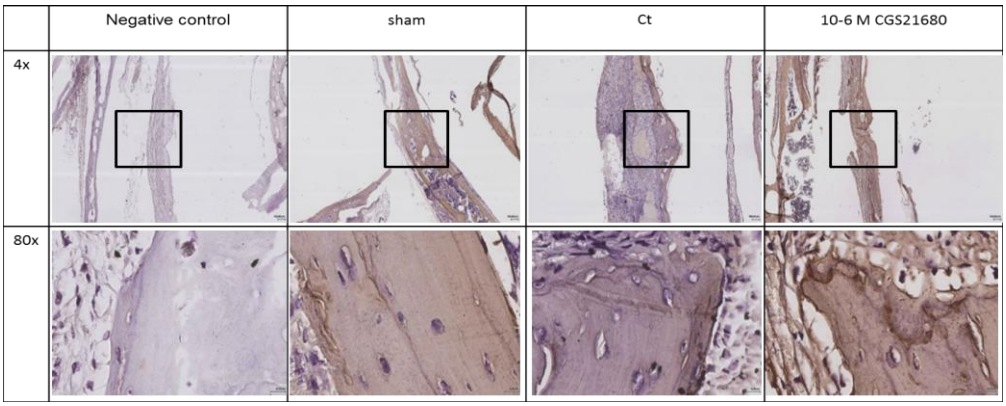

B.

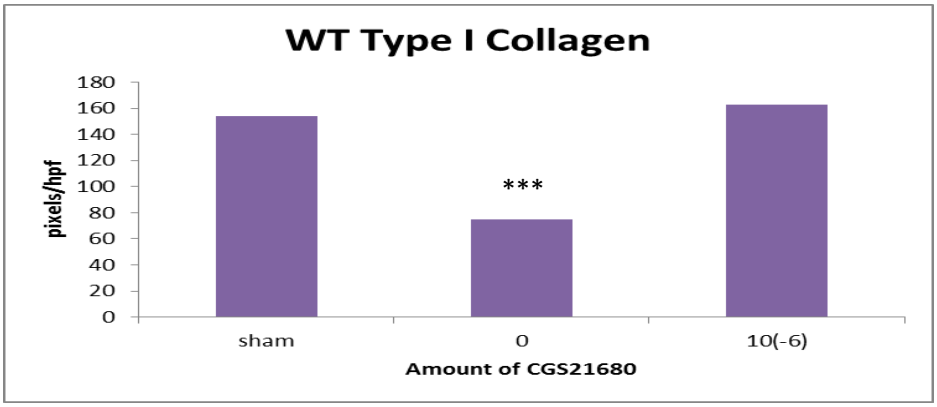

C.

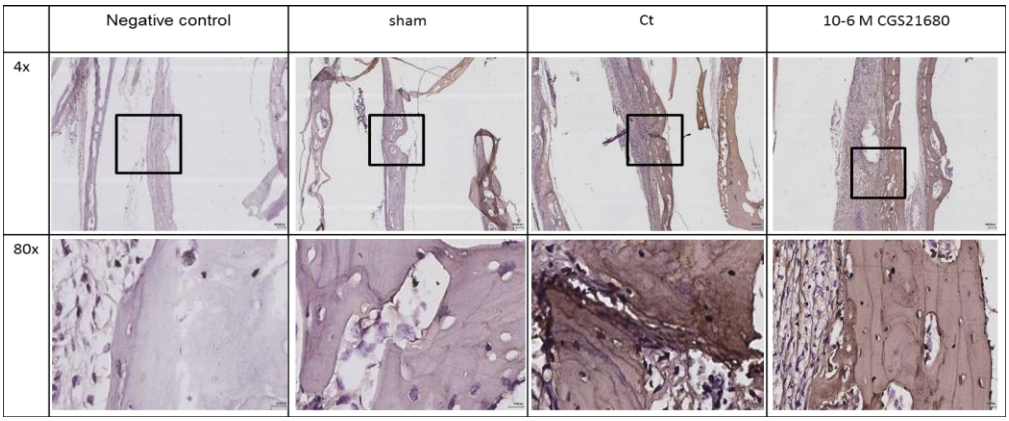

D.

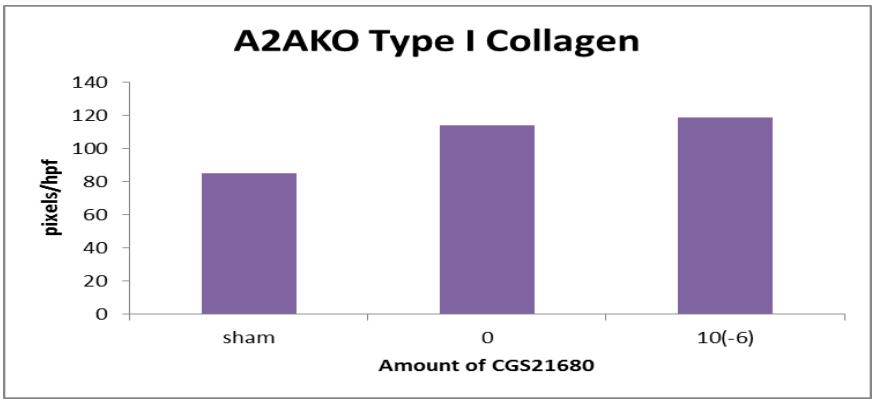

Figure 11: Immunohistochemistry for osteoblast marker: Type I collagen in WT and A_{2A}KO mice. (**A**) Calvaria were prepared and immunohistologic staining was processed on sham or UHMWPE-exposed WT mice, treated with saline or CGS21680 (1µm). The sections shown are representative of calvaria stained for type I collagen. All images from slides were taken at the magnifications: 4x and 80x. Scale bars100 µm for 4x and 10 µm for 80x. (**B**) Immunohistochemistry quantifications of pixels/hpf for (A). Data are means ± SEM for 3 different slides per untreated mouse (n=5), and each mouse treated with particulate and saline (n=5) or particulate and 1 µm of CGS21680 (n=5). (**C**) Calvaria were prepared and immunohistologic staining was processed on sham or UHMWPE-exposed WT mice, treated with saline or CGS21680 (1um). The sections shown are representative of calvaria (from n=3 mice) stained for type I collagem. All images were taken at the magnifications: 4x and 80x. Scale bars100 µm for 4x and 10 µm for 80x. (**D**) Immunohistochemistry quantifications of pixels/hpf for (C) analyzed by SigmaScan. Data are means ± SEM for 3 different slides per untreated mouse (n=5), and each mouse treated with particulate and saline (n=5) or particulate and 1 µm of CGS21680 (n=5). *P<0.5;**P<0.01; ***P< 0.001, compared to sham, ANOVA.

From (figure 11), the number of positive OBs could not be counted with a human type I collagen primary AB staining like the other ABs used in this project. This human type I collagen primary AB stained the whole calvaria. There is a difference in the brown color intensity for the slides of different treatments. The software SigmaScan was used to calculate the number of pixels/hpf of brown coloration from the immunostaining of the

calvaria. The results from (figure 11 A-B) show that the brown color intensity decreased from 154 pixels/hpf for the WT non-treated mice calvaria to 75 pixels/hpf (***P<0.001 compared WT sham) for the WT mice calvaria in presence of wear particles and treatment with PBS. For the WT calvaria in presence of wear particles and treatment of 10^{-6} M CGS21680, the brown color intensity increased to 163 pixels/ hpf at the site of incision of UHMWPE compared to treatment with PBS. From (figure 11 C-D), the A_{2A}KO mice slides show no significant difference in the number of positive OBs between the A_{2A}KO with the non-treated mice to the control mice and the 10^{-6} M CGS21680 treated mice.

4.1.2.4. RANK

A.

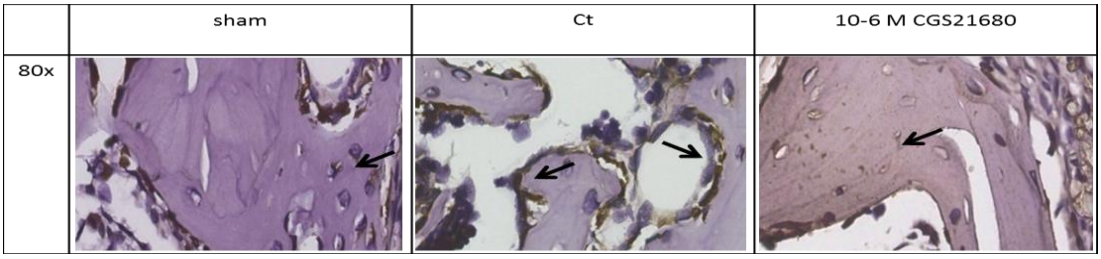

B.

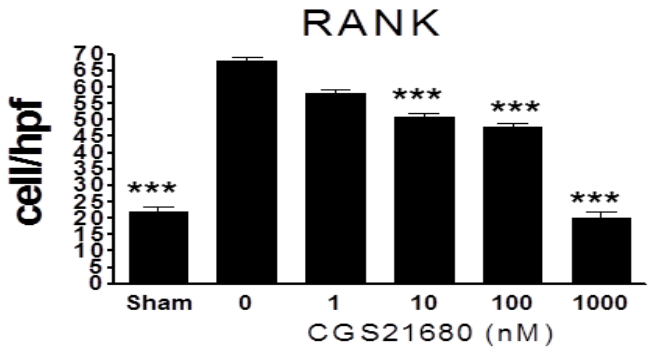

C.

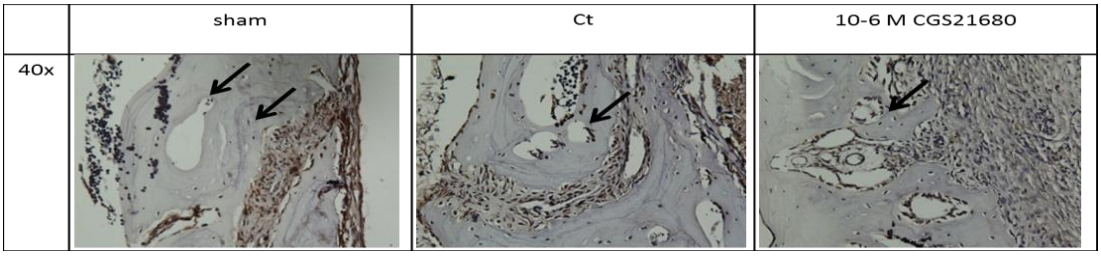

D.

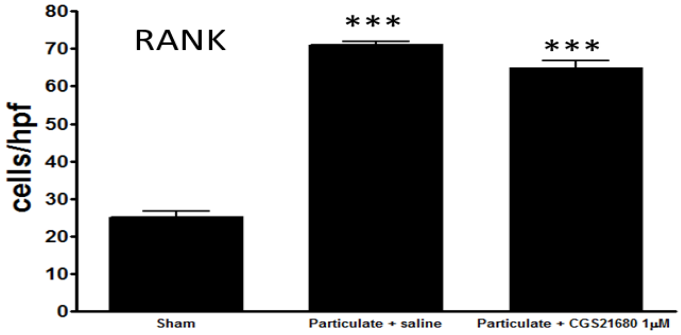

Figure 12: Immunohistochemistry for osteoclast marker: RANK in WT and A_{2A}KO mice.
(**A**) Calvaria were prepared and immunohistologic staining was processed on sham or UHMWPE-exposed WT mice, treated with saline or CGS21680 (1µm). The sections shown are representative of calvaria stained for RANK. All images from slides were taken at the magnifications: 4x and 80x. Scale bars100 µm for 4x and 10 µm for 80x. (**B**) Immunohistochemistry quantifications of cells/hpf for (A). Data are means ± SEM for 3 different slides per untreated mouse (n=5), and each mouse treated with particulate and saline (n=5) or particulate and 1 µm of CGS21680 (n=5).(**C**) Calvaria were prepared and immunohistologic staining was processed on sham or UHMWPE-exposed WT mice, treated with saline or CGS21680 (1um). The sections shown are representative of calvaria (from n=3 mice) stained for RANK. All images were taken at the magnifications: 4x and 80x. Scale bars100 µm for 4x and 10 µm for 80x. (**D**) Immunohistochemistry quantifications of cells/hpf for (C). Data are means ± SEM for 3 different slides per untreated mouse (n=5), and each mouse treated with particulate and saline (n=5) or particulate and 1 µm of CGS21680 (n=5). *P<0.5;**P<0.01; ***P< 0.001, compared to control for (B) and compared to sham for (D), ANOVA.

From (figure 12 A-B), a RANK primary AB staining shows that the WT non-treated mice had an average of 22 ± 1 positive OCs (with ***P<0.001 compared to the WT control mice). For the WT mice calvaria in presence of wear particles and treatment with PBS, there was an increase in the average of positive OCs to 67 ± 2 compared to sham. The WT mice treated with1000 nM of CGS21680 had a decrease to 20 ± 2 of the number of positive OCs (with ***P<0.001 compared to the WT control mice) at the site of incision of UHMWPE compared to the control mice treated with PBS. In (figure 12 B), there is a dose response done with CGS21680 which shows the effects of the A_{2A}R agonist from 10^{-6} M to 10^{-9} M, showing less positive OCs correlating to higher concentrations of the A_{2A}R agonist. In (figure 12 C-D), the A_{2A}KO mice slides show a statistical significant change in the number of positive OCs for the control and CGS21680 treated mice compared to the non-treated mice.

4.1.2.5. RANKL

A.

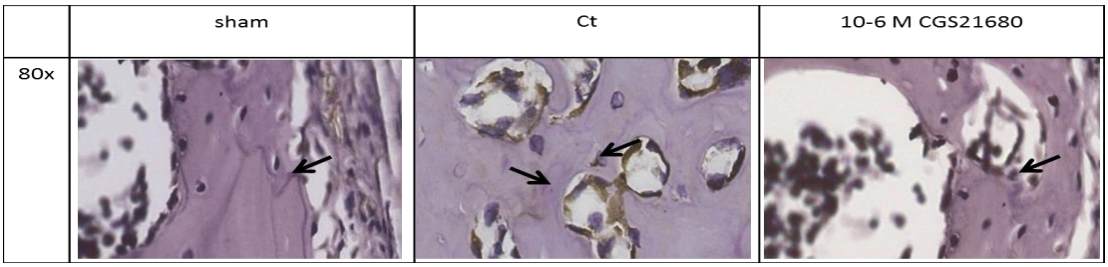

B.

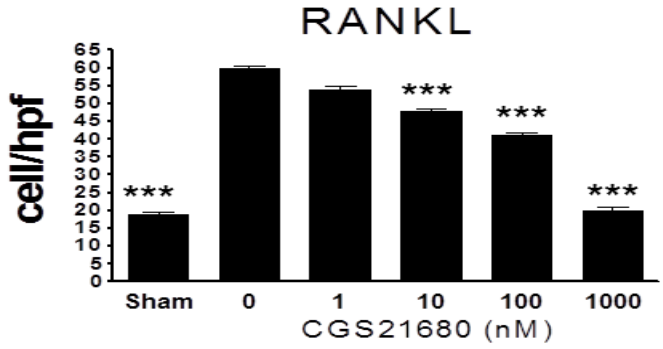

C.

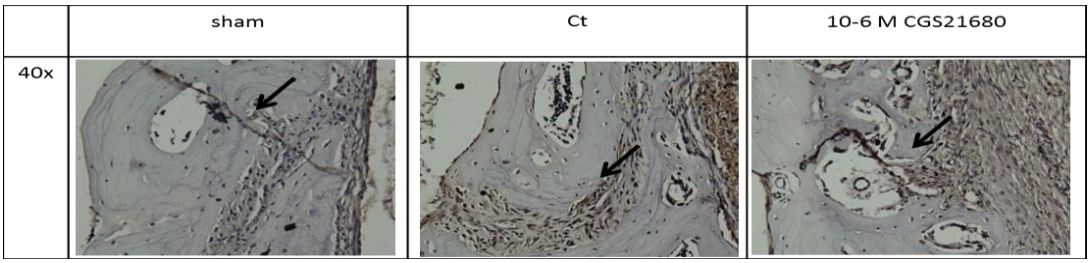

D.

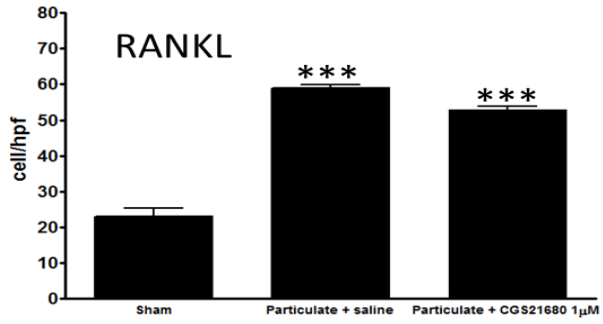

Figure 13: Immunohistochemistry for osteoclast marker: RANKL in WT and A_{2A}KO mice.
(**A**) Calvaria were prepared and immunohistologic staining was processed on sham or UHMWPE-exposed WT mice, treated with saline or CGS21680 (1µm). The sections shown are representative of calvaria stained for RANKL. All images from slides were taken at the magnifications: 4x and 80x. Scale bars100 µm for 4x and 10 µm for 80x. (**B**) Immunohistochemistry quantifications of cells/hpf for (A). Data

are means ± SEM for 3 different slides per untreated mouse (n=5), and each mouse treated with particulate and saline (n=5) or particulate and 1 µm of CGS21680 (n=5).(**C**) Calvaria were prepared and immunohistologic staining was processed on sham or UHMWPE-exposed WT mice, treated with saline or CGS21680 (1um). The sections shown are representative of calvaria (from n=3 mice) stained for RANKL. All images were taken at the magnifications: 4x and 80x. Scale bars100 µm for 4x and 10 µm for 80x. (**D**) Immunohistochemistry quantifications of cells/hpf for (C). Data are means ± SEM for 3 different slides per untreated mouse (n=5), and each mouse treated with particulate and saline (n=5) or particulate and 1 µm of CGS21680 (n=5). *P<0.5;**P<0.01; ***P< 0.001, compared to control for (B) and compared to sham for (D), ANOVA.

From (figure 13 A-B), a RANKL primary AB staining shows that the WT non-treated mice had an average of 19 ± 1 positive OCs (with ***P<0.001 compared to the WT control mice). For the WT mice calvaria in presence of wear particles and treatment with PBS, there was an increase in the average of positive OCs to 60 ± 1 compared to sham. The WT mice treated with1000 nM of CGS21680 had a decrease to 21 ± 3 of the number of positive OCs (with ***P<0.001 compared to the WT control mice) at the site of incision of UHMWPE compared to the WT control mice treated with PBS. In (figure 13 B), there is a dose response done with CGS21680 which shows the effects of the $A_{2A}R$ agonist from 10^{-6} M to 10^{-9} M, showing less positive OCs correlating to higher concentrations of the $A_{2A}R$ agonist. In (figure 13 C-D), the $A_{2A}KO$ mice slides show a statistical significant change in the number of positive OCs for the control and the CGS21680 treated mice compared to the non-treated group in $A_{2A}KO$ mice.

4.1.2.6. Osteoprotegerin

A.

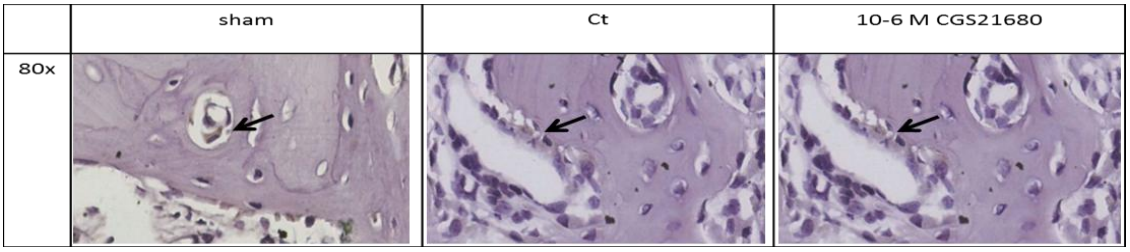

B.

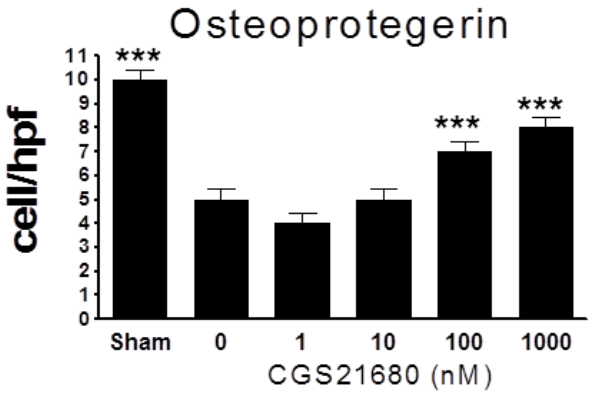

C.

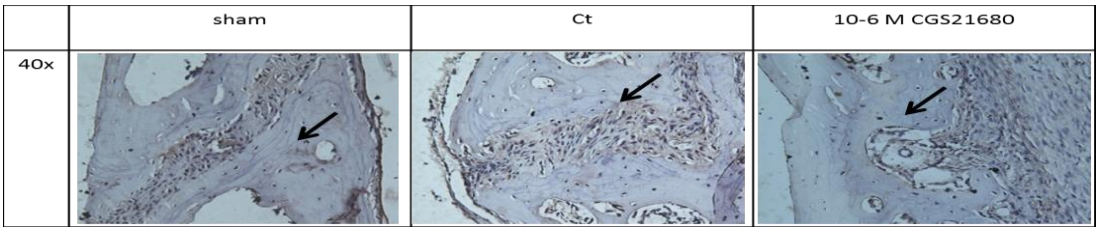

D.

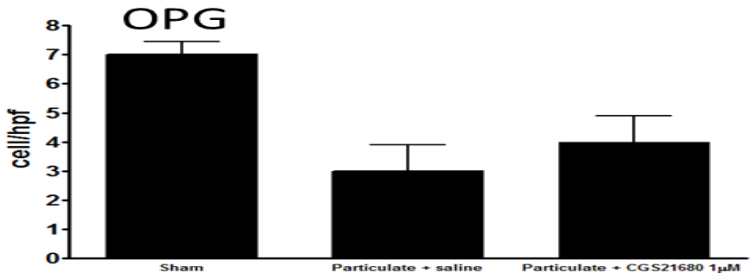

Figure 14: Immunohistochemistry for osteoblast marker: OPG in WT and A_{2A}KO mice.
(**A**) Calvaria were prepared and immunohistologic staining was processed on sham or UHMWPE-exposed WT mice, treated with saline or CGS21680 (1µm). The sections shown are representative of calvaria stained for OPG. All images from slides were taken at the magnifications: 4x and 80x. Scale bars100 µm for 4x and 10 µm for 80x. (**B**) Immunohistochemistry quantifications of cells/hpf for (A). Data are means ± SEM for 3 different slides per untreated mouse (n=5), and each mouse treated with particulate and saline (n=5) or particulate and 1 µm of CGS21680 (n=5).(**C**) Calvaria were prepared and immunohistologic staining was processed on sham or UHMWPE-exposed WT mice, treated with saline or CGS21680 (1um). The sections shown are representative of calvaria (from n=3 mice) stained for OPG. All images were taken at the magnifications: 4x and 80x. Scale bars100 µm for 4x and 10 µm for 80x. (**D**) Immunohistochemistry quantifications of cells/hpf for (C). Data are means ± SEM for 3 different slides per untreated mouse (n=5), and each mouse treated with particulate and saline (n=5) or particulate and 1 µm of CGS21680 (n=5). *P<0.5;**P<0.01; ***P< 0.001, compared to control for (B) and compared to sham for (D), ANOVA.

From (figure 14 A-B), an OPG primary AB staining show that the WT non-treated mice had an average of 10 ± 2 positive OBs (with ***P<0.001 compared to the WT control

mice). For the WT mice calvaria in presence of wear particles and treatment with PBS, there was a decrease in the average of OBs to 5 ± 2 compared to sham. The WT mice treated with1000 nM of CGS21680 had an increase to 8 ± 2 of the number of positive OBs (with ***P<0.001 compared to the WT control mice) at the site of incision of UHMWPE compared to the WT control mice treated with PBS. In (figure 14 B), there is a dose response done with CGS21680 which shows the effects of the $A_{2A}R$ agonist from 10^{-6} M to 10^{-9} M, showing less positive OBs correlating to lower concentrations of the $A_{2A}R$ agonist. In (figure 14 C-D), the $A_{2A}KO$ mice slides show no statistical significant change in the number of positive OBs for the control and the CGS21680-treated mice compared to the non-treated mice.

4.1.2.7. Osteopontin

A.

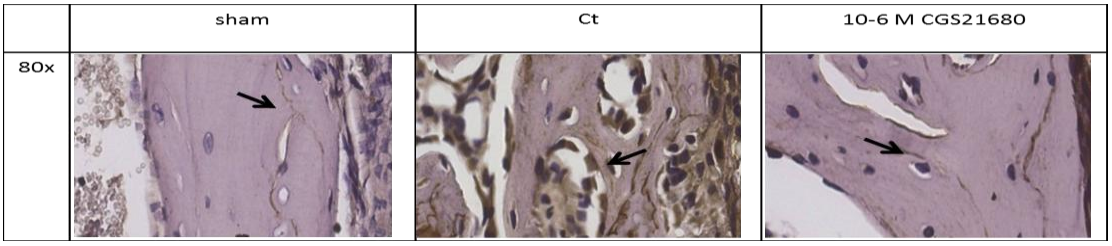

B.

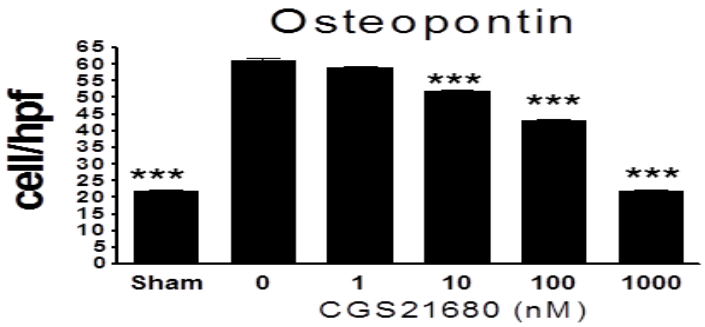

C.

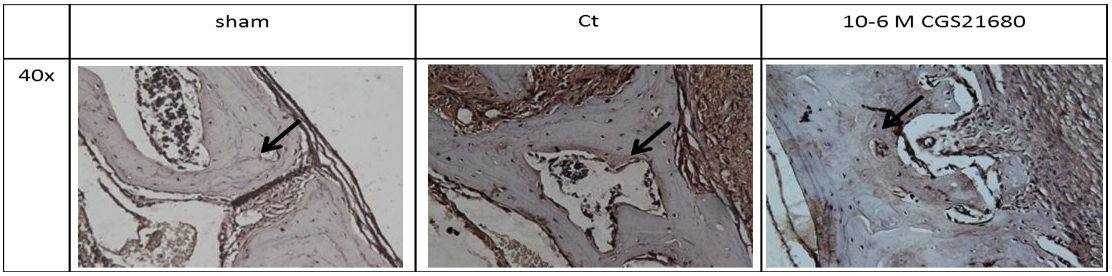

D.

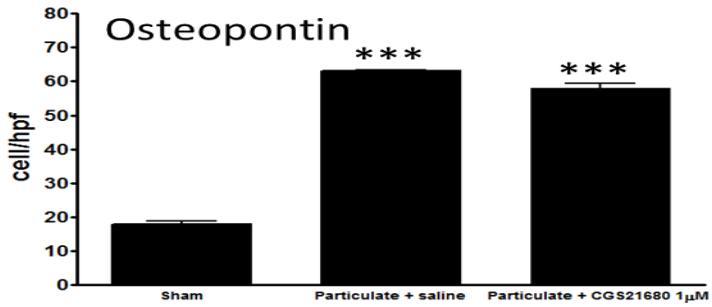

Figure 15: Immunohistochemistry for osteoclast marker: Osteopontin in WT and A_{2A}KO mice.
(**A**) Calvaria were prepared and immunohistologic staining was processed on sham or UHMWPE-exposed WT mice, treated with saline or CGS21680 (1μm). The sections shown are representative of calvaria stained for Osteopontin. All images from slides were taken at the magnifications: 4x and 80x. Scale bars100 μm for 4x and 10 μm for 80x. (**B**) Immunohistochemistry quantifications of cells/hpf for (A). Data are means ± SEM for 3 different slides per untreated mouse (n=5), and each mouse treated with particulate and saline (n=5) or particulate and 1 μm of CGS21680 (n=5).(**C**) Calvaria were prepared and immunohistologic staining was processed on sham or UHMWPE-exposed WT mice, treated with saline or CGS21680 (1um). The sections shown are representative of calvaria (from n=3 mice) stained for Osteopontin. All images were taken at the magnifications: 4x and 80x. Scale bars100 μm for 4x and 10 μm for 80x. (**D**) Immunohistochemistry quantifications of cells/hpf for (C). Data are means ± SEM for 3 different slides per untreated mouse (n=5), and each mouse treated with particulate and saline (n=5) or particulate and 1 μm of CGS21680 (n=5). *P<0.5;**P<0.01; ***P< 0.001, compared to control for (B) and compated to sham for (D), ANOVA.

From (figure 15 A-B), an Osteopontin primary AB staining show that the WT non-treated mice had an average of 22 ± 1 positive OCs (with ***P<0.001 compared to the WT control mice). For the WT mice calvaria in presence of wear particles and treatment with PBS, there was an increase in the average of positive OCs to 63 ± 2 compared to sham. The WT mice treated with 1000 nM of CGS21680 had a decrease to 19 ± 1 of the number of positive OCs (with ***P<0.001 compared to the WT control mice) at the site of incision of UHMWPE compared to the control mice treated with PBS. In (figure 15 B), there is a dose response done with CGS21680 which shows the effects of the A_{2A}R agonist from 10^{-6} M to 10^{-9} M, showing less positive OCs correlating to higher concentrations of the A_{2A}R agonist. In (figure 15 C-D), the A_{2A}KO mice slides show a statistical significant change in the number of positive OCs for the control and CGS21680-treated mice compared to the non-treated group in A_{2A}KO mice.

4.1.2.8. Osteocalcin

A.

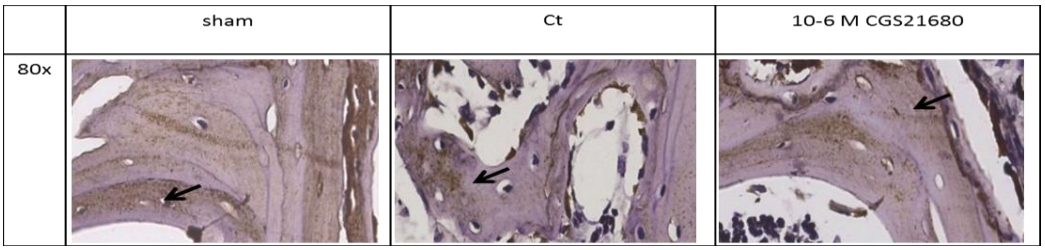

B.

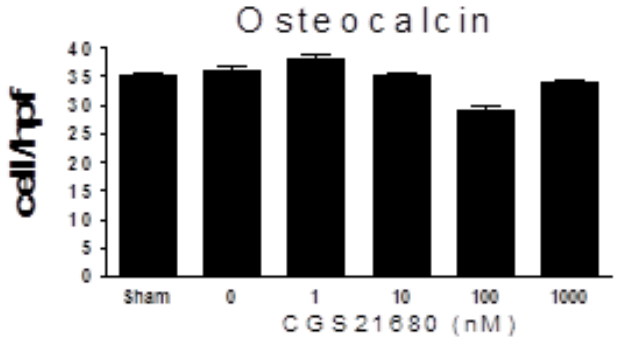

C.

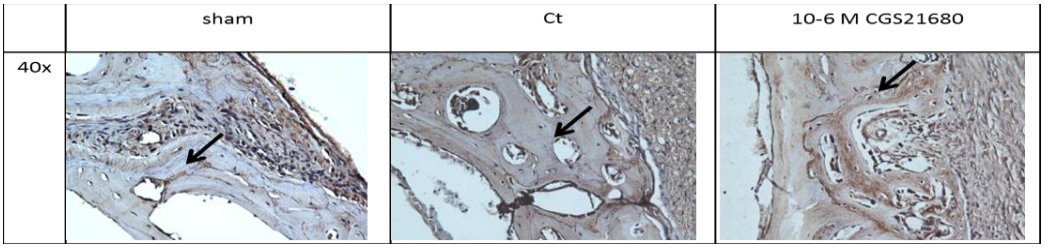

D.

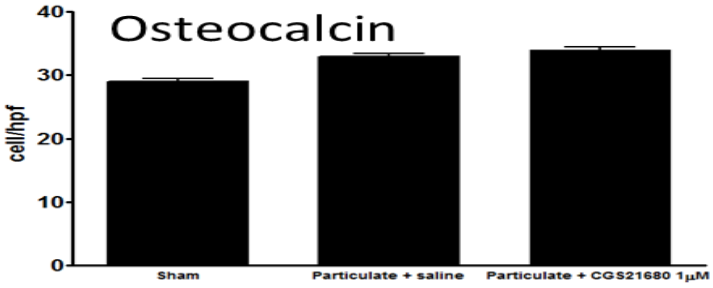

Figure 16: Immunohistochemistry for osteoblast marker: Osteocalcin in WT and A_{2A}KO mice.
(**A**) Calvaria were prepared and immunohistologic staining was processed on sham or UHMWPE-exposed WT mice, treated with saline or CGS21680 (1µm). The sections shown are representative of calvaria stained for Osteocalcin. All images from slides were taken at the magnifications: 4x and 80x. Scale bars100 µm for 4x and 10 µm for 80x. (**B**) Immunohistochemistry quantifications of cells/hpf for (A). Data are means ± SEM for 3 different slides per untreated mouse (n=5), and each mouse treated with

particulate and saline (n=5) or particulate and 1 µm of CGS21680 (n=5).(**C**) Calvaria were prepared and immunohistologic staining was processed on sham or UHMWPE-exposed WT mice, treated with saline or CGS21680 (1um). The sections shown are representative of calvaria (from n=3 mice) stained for Osteocalcin. All images were taken at the magnifications: 4x and 80x. Scale bars100 µm for 4x and 10 µm for 80x. (**D**) Immunohistochemistry quantifications of cells/hpf for (C). Data are means ± SEM for 3 different slides per untreated mouse (n=5), and each mouse treated with particulate and saline (n=5) or particulate and 1 µm of CGS21680 (n=5). *P<0.5;**P<0.01; ***P< 0.001, compared to control for (B) and compated to sham for (D), ANOVA.

From (figure 16 A-B), an Osteocalcin primary AB staining show that the WT non-treated mice had an average of 35 ± 1 positive OBs, similar values to the WT control mice with an average of 36 ± 2 positive OBs in presence of wear particles and also to the WT CGS21680-treated mice with an average of 33 ± 1 positive OBs. There was no statistical significant difference in the number of positive OBs between the different treatments when using osteocalcin in this experiment. CGS21680 had no effect on the number of positive OBs at the site of incision of UHMWPE compared to the WT control mice treated with PBS. In (figure 16 B), there is a dose response done with CGS21680 which shows no effect of the $A_{2A}R$ agonist from 10^{-6} M to 10^{-9} M. In (figure 16 C-D), the $A_{2A}KO$ mice slides show no statistical significant change in the number of positive OBs for the control and the CGS21680-treated mice compared to the non-treated group in $A_{2A}KO$ mice.

4.2. In vitro studies

4.2.1. Analysis of calcific deposition by differentiated osteoblasts with Alizarin Red Staining

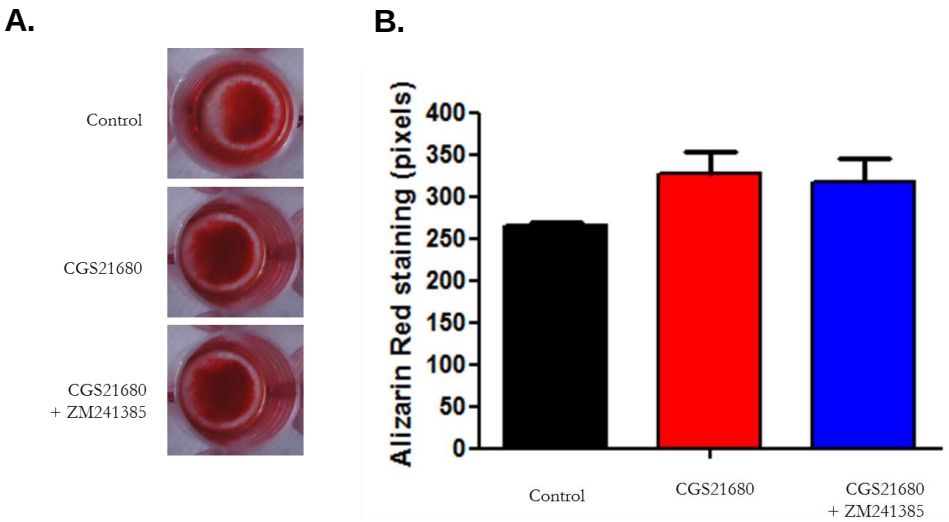

Figure 17: Effect of osteolysis on osteoblast formation by mice bone marrow cells.

(A) *Mice primary bone marrow mesenchymal stem cells were fixed and stained with Alizarin red staining after differentiation into OBs for 10 days with no treatment, treatment with A_{2A} receptor agonist 1 μM CGS2168 or pretreatment with 1 μM ZM241385 and 1 μM CGS21680 treatment. Alizarin red staining positive OBs are colored red* ***(B)*** *The number of Alizarin red staining positive OBs for each treatment was determined by the red color intensity counted in pixels.*

According to the graph, when pre-OBs were treated with A_{2A}R agonist CGS21680 their differentiation into OBs slightly increased with higher red color intensity compared to the non-treated OBs. The pre-OBs pre-treated with A_{2A}R antagonist ZM241385 and treated with CGS21680 showed similar red color intensity to the CGS21680-treated OBs marking no statistically significant difference in the calcific deposition by the differentiated OBs.

4.2.2. RANKL and OPG expression on messenger level with RT-PCR

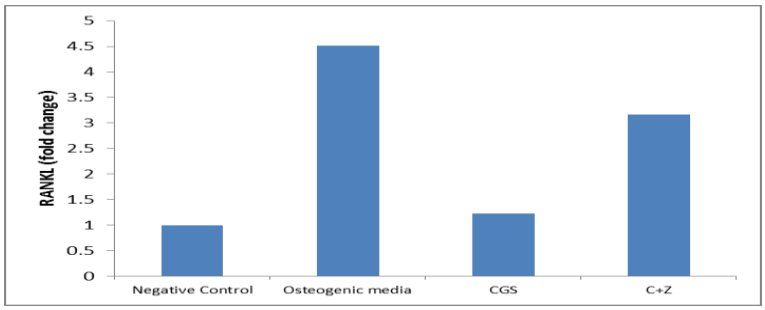

Graph 1: Result from RT-PCR with RANKL secretion from OB with housekeeping gene GAPDH

According to this graph, the OB differentiation with osteogenic media stimulated an increase in RANKL gene expression to 4.5 fold change compared to the control taken from non differentiated OBs at 1 fold change. When the OBs were differentiated and treated with $A_{2A}R$ agonist, 10^{-6} M CGS21680, the RANKL gene expression by OBs decreased to 1.2 fold change. The RANKL gene expression by OBs was increased when OBs differentiated and were pretreated with $A_{2A}R$ antagonist, 10^{-6} M ZM241385 to 3.2 fold change.

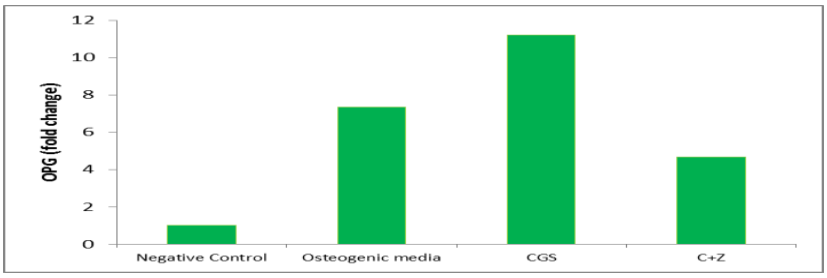

Graph 2: Result from RT-PCR with OPG secretion from OB with housekeeping gene GAPDH

According to this graph, the OB differentiation with osteogenic media stimulated an OPG gene expression increase to 7.4 fold change compared to the control taken from non differentiated cells with 1 fold change. When the OBs were differentiated and treated with $A_{2A}R$ agonist, 10^{-6} M CGS21680, the OPG gene expression by OBs increased to 11.2 fold change. The OPG gene expression by OBs was decreased when

OBs differentiated and were pretreated with $A_{2A}R$ antagonist, 10^{-6} M ZM241385 to 4.7 fold change.

5. Discussion

5.1. In-vivo studies

5.1.1. Bone formation is decreased during osteolysis

In the presence of wear particles, bone formation decreased. The $A_{2A}R$ activation with $A_{2A}R$ agonist, CGS26180, prevented OC differentiation and promoted bone formation increase (figure 7). It is likely that $A_{2A}R$ agonist, CGS26180, promoted the OB differentiation. When the mice were injected locally with PBS, the OB activity showed lower than the mice injected with CGS21680 by in-vivo imaging after Xenolight injection.

5.1.2. Bone resoption and formation markers in osteolysis model with IHC

Alkaline phosphatase, Osteonectin, Type I collagen, OPG and Osteocalcin are bone formation markers. RANK, RANKL and Osteopontin are bone resorption markers.

Alkaline phosphatase is an important protein expressed in bone and contributes to the hard tissue formation [15].

Osteonectin is a glycoprotein which has a crucial role in bone mineralization. It is a bone-specific protein which binds selectively to hydroxyapatite and collagen. The complex binds synthetic apatite crystals and free calcium ions when bound to insolubilized type I collagen. Osteonectin links the bone mineral and collagen phases and might initiate active mineralization in normal skeletal tissue [16]. SPARC (secreted protein acidic and rich in cysteine) is identical to osteonectin, which is also an important protein in bone calcification and highly conserved between species. SPARC is a matricellular protein that is highly expressed by bone cells[17]. SPARC was the primary AB used in the experiment.

Type I collagen is the most abundant type of collagen. Being the major protein in bone, it is widely distributed in almost all connective tissues. It represents approximately 95%

of the entire collagen content of bone and about 80% of the total proteins present in bone [18].

Notice: The AB used in this experiment was a human type I collagen, which was not 100 % validated for mice. This AB was used due to lack of time and alternatives with Hurricane Sandy.

OPG is an OB secreted protein which acts as a decoy receptor for RANKL. OPG blocks RANK/RANKL interaction by binding to RANKL and prevents OCs differentiation and activation [9]. OPG is therefore an antiosteoclastogenic bone formation marker.

Osteocalcin is the most abundant OB-specific non-collagenous protein of the bone ECM [19]. Represents 1-2% of total bone protein, it also binds strongly to apatite and calcium [20]. Osteocalcin can directly stimulate adipocytes to regulate insulin sensitivity. It is a determinant of bone formation [21].

Osteopontin is an extracellular matrix protein that favours osteoclast ruffled borders development and colocalizes with osteoclast on the surface of bone [4]. Osteopontin is secreted by OB. Osteopontin is a highly phosphorylated sialoprotein that is a prominent component of the mineralized extracellular matrices of bones and teeth [22]. In this experiment, osteopontin acted as a bone resorption marker.

RANKL is a TNF super family member. It is a surface molecule expressed by a large set of different cell types including pre-OBs and activated T-cells. RANKL enables OC differentiation and activation upon binding with its receptor RANK on pre-OC surface. RANKL increases the ability of dendritic cells to stimulate naïve T-cell proliferation [20, 23]. Therefore, there is a correlation between the OC differentiation and inflammation caused by the wear debris.

From figures (9, 10, 11, 14), it is possible to observe that in WT mice the treatment of $A_{2A}R$ agonist in the osteolysis model enhanced bone formation. The immunostaining

from (figure 16) showed that osteocalcin had no effect upon A_{2A}R agonist, CGS21680 treatment, indicating no reaction in bone formation. Similar results to the the other bone formation markers were expected, there should have been an increase in bone formation when staining with osteocalcin and treating with A_{2A}R agonist. A problem might have occurred with the osteocalcin primary AB. The A_{2A}KO mice results showed that with the primary ABs used: Alkaline phosphatase, Type I Collagen, OPG, Osteocalcin had no statistical significant differences between sham and the control mice or the CGS21680-treated mice. A_{2A}KO mice results showed that when Osteonectin was used as a primary AB, there was a statistical significant difference between the non-treated and the control mice. When osteonectin was used, the A_{2A}KO mice treated with CGS21680 had similar values to the non-treated mice, relating to a statistically significant difference between the control mice and the CGS21680 treated mice when wear particles were applied to these mice calvaria. This result is unexpected as CGS21680 should have no effect in A_{2A}KO mice. This controversial result was highly due to technical errors. The standard deviation to the alkaline phosphatase, type I collagen and osteonectin results were high. (*Notice: The experiments could not be repeated)*. From figures (12, 13, 15), it is possible to observe that in WT mice the treatment of A_{2A}R agonist in the osteolysis model decreased bone resorption on the bone calvaria. This is similar to the results from previous studies done showing A_{2A} receptor activation prevents wear particle-induced osteolysis [4]. The A_{2A}KO mice results showed that the primary ABs used: RANK, RANKL and Osteopontin had statistical significant differences between the non-treated and the control, also the CGS21680-treated mice.

CGS21680 is the most commonly used agonist for A_{2A}R activation. It is the standard A_{2A} radioligand in its tritium-labeled form. CGS21680 is A_{2A}-selective in rat, however it shows high affinity for the human A_3 receptor and low selectivity human A_{2A}R [12]. Different A_{2A}-selective agonists have been developed such as Regadenoson or Apadenoson. Several other A_{2A}-selective agonists are being or have been clinically evaluated. The statistical significance differences of the number of positive OBs for the bone formation markers and of the positive OCs for the bone resorption markers of the

A_{2A}KO control mice and A_{2A}KO CGS21680-treated mice was compared to the A_{2A}KO non-treated mice. The A_{2A}KO PBS-treated mice with wear particles and the A_{2A}KO 10^{-6} M CGS21680-treated mice with wear particles did not show much difference among each other, but generally with the A_{2A}KO non-treated mice. A_{2A}KO mice should demonstrate that the bone resorption inhibitory effect of CGS1680 is lost when the A2AR is deleted, even in an osteolysis model. A_{2A}R losses its pharmacological effect in A_{2A}RKO [12].

While studying the mice calvaria through IHC, A_{2A}R activation with A_{2A}R agonist CGS21680 showed a decrease in OC differentiation favoring an increase in bone formation.

5.2. In-vitro studies

5.2.1. Bone formation is indirectly increased by A_{2A}R activation by analyzing the calcific deposition of osteoblasts with Alizarin Red Staining

Matrix mineralization is a direct effect of OB function and is a measurement to OB differentiation. When bone marrow derived primary cells from the mice femur and tibia were differentiated and treated with A_{2A}R agonist, the calcific deposition by these differentiated and CGS21680-treated OBs increased compared to the non-treated differentiated OBs, this was shown by a higher red color intensity of the calcific deposition by the differentiated non-treated OBs. The bone mineralization from bone marrow derived primary cells from the mice femur and tibia differentiated and pretreated with A_{2A}R antagonist and agonist showed similar red color intensity to the differentiated CGS21680-treated OBs. The difference in matrix mineralization between the A_{2A}R agonist and antagonist treatments to the differentiated OBs was not statistically significant. The OBs were indirectly affected by the A_{2A}R agonist and antagonist. This shows that bone formation is not increased upon A_{2A}R activation on OBs but upon the crosstalk between OBs and OCs. The decrease of the number of differentiated OCs induces secretion of cytokines that leads to OB differentiation activation.

More alizarin red staining experiments were performed with the mice bone marrow derived differentiated OBs but the results were not revealing as the staining washed away during the rinsing steps. This might be caused by manipulation or storage errors. It is possible that the OBs did not attach properly to the wells also due to an improper pH of the Alizarin red staining solution which is critical because cell adhesion is a pH-dependent phenomenon [24].

Notice: A dose response of the $A_{2A}R$ agonist and antagonist was on-going but this was lost during Hurricane Sandy.

5.2.2. RANKL and OPG expression on messenger level with RT-PCR shows the importance of the cross talk between bone formation and bone resorption

RANKL is secreted by OBs in response to osteotropic factors such as vitamin D, PTH and prostaglandins. Inflammatory cytokines such as TNF, IL-1 and IL-17 can induce RANKL expression [20, 25-27]. RANKL is essential for OC differentiation and bone-resorbing capacity by binding to its receptor RANK on OC-precursor cells. The interaction of RANKL with RANK is modulated by OPG, a secreted glycoprotein which was identified as a decoy soluble factor that strongly suppresses OC differentiation in vivo and in vitro.

The $A_{2A}R$ activation upon CGS21680 treatment induced an increase of OPG secretion by OBs; this was reverted by pretreatment with ZM241385. OBs secreted more OPG to prevent differentiation of OCs when $A_{2A}R$ were activated with CGS21680 and secreted less OPG when $A_{2A}R$ were inactivated with ZM241385 to allow OC differentiation.

The $A_{2A}R$ activation upon CGS21680 treatment induced a decrease of RANKL secretion by OBs; this was reverted by pretreatment with ZM241385. OBs secreted more RANKL to enable differentiation of OCs when $A_{2A}R$ were inactivated with ZM241385 and secreted less RANKL when $A_{2A}R$ were activated with CGS21680 to prevent OC differentiation.

With the $A_{2A}R$ agonist and antagonist treatments, it was possible to observe that according to the activation and inactivation of the $A_{2A}Rs$, OPG and RANKL secretions were modified and therefore there were opposite effects on OCs differentiation. These OCs send signals to balance bone homeostasis. In the osteolysis model, the activation with $A_{2A}R$ agonist CGS21680 indirectly increased the number of differentiated OBs by inhibiting the OCs differentiation. The inactivation with $A_{2A}R$ antagonist ZM241385 indirectly decreased the number of differentiated OBs by stimulating the OCs differentiation.

Notice: No statistical analysis could be done with the RT-PCR results because this experiment was done once with the appropriate conditions. Other trials were subject to contaminations or complications. This led to some inadequate results from the RT-PCR. To have a clearer idea of the cross talk between OBs and OCs, different time points were going to be done (24h, 48h, 5 days and 10 days). This could not be processed due to losses caused by Hurricane Sandy. The only time point samples that were saved were the 10 day-differentiated OBs. A western blot for protein analysis was also planned, but could not be performed for the same reasons.

The central role of the RANKL-RANK-OPG signaling pathway in bone resorption also triggered researchers´ increasing interest in therapeutic targeting of this system in human diseases and recent clinical trials on postmenopausal osteoporosis which have revealed the potent anti-resorptive effect of a neutralizing RANKL AB (denosumab). In our project WT male mice were used in the in-vivo studies and WT female mice were used in the in-vitro studies. OPG expression is induced by estrogens, which explains the increase in OC numbers and enhanced bone resoprtion during menopause when women´s level of estrogen naturally decreases. RANKL deficient mice display severe osteopetrosis due to the lack of OC formation [28].

Due to the importance of coupling between OBs and OCs to balance bone homeostasis, wear particles induced OC-mediated bone resorption decreased the number of differentiated OBs and $A_{2A}R$ activation reverted this effect.

Entire bone remodeling process takes 3 to 6 months. Adults continuously remodel their entire skeleton in 7 to 10 years [9]. Proper coupling between bone formation and bone resorption is essential to maintain bone integrity. Under normal conditions, there are two main regulating mechanism involved in coupling: the expression of essential pro-osteoclastogenic cytokines by the OB lineage and the ephrin ligand/ ephrin receptor bidirectional signaling. [29, 30]. When OBs differentiate, the key transcription factors Runx2 and Osterix 1 induce the differentiation of the MSCs into OBs in response to external stimuli [31]. In response to Wnt signaling, OBs slowly lose their supportive activity for OCs when maturing toward more mineralizing cells and become bon-embedded osteocytes. OBs secrete antiosteoclastogenic molecules such as OPG and Wnt inhibitors sclerostin, dickkopf-1 and secreted frizzled related protein 1 (SFRP1) which either block OC differentiation or inhibit further differentiation of OBs [9]. Bone remodeling is regulated locally but also by various systemic hormonal pathways including the sex and growth hormone: GH and IGF axes. Two major systemic neuroendocrine regulators (osteocalcin and leptin) of bone homeostasis co-regulate bone, fat and energy metabolism [32].

6. **Conclusion**

A_{2A} receptor agonist, CGS21680, prevents osteoclast differentiation. As more osteoclasts differentiate in presence of wear particles, less osteoblast differentiate because osteoclast and osteoblast formation should remain in balance. The in-vivo and in-vitro studies in this project demonstrated that wear particles-induced osteolysis decreased bone formation. However, the A_{2A} receptor activation indirectly increased bone formation in the osteolysis model through the prevention of osteoclast differentiation. A_{2A} receptor activation in an osteolysis model prevents osteoclastogenesis and indirectly stimulates osteoblastogenesis. After thus discovery, can A_{2A} receptor activation with A_{2A} receptor agonist lead to bone formation on the surface of hip implants to help improve THA long term patient outcomes?

7. References

1. **Berry, D.J., et al., *Twenty-five-year survivorship of two thousand consecutive primary Charnley total hip replacements: factors affecting survivorship of acetabular and femoral components.* J Bone Joint Surg Am, 2002. 84-A(2): p. 171-7.**
2. **Abu-Amer, Y., I. Darwech, and J.C. Clohisy, *Aseptic loosening of total joint replacements: mechanisms underlying osteolysis and potential therapies.* Arthritis Res Ther, 2007. 9 Suppl 1: p. S6.**
3. **van der Veen, H.C., et al., *Wear, bone density, functional outcome and survival in vitamin E-incorporated polyethylene cups in reversed hybrid total hip arthroplasty: design of a randomized controlled trial.* BMC Musculoskelet Disord, 2012. 13(1): p. 178.**
4. **Mediero, A., et al., *Adenosine A2A receptor activation prevents wear particle-induced osteolysis.* Sci Transl Med, 2012. 4(135): p. 135ra65.**
5. **Saleh, K.J., I. Thongtrangan, and E.M. Schwarz, *Osteolysis: medical and surgical approaches.* Clin Orthop Relat Res, 2004(427): p. 138-47.**
6. **Bozic, K.J., et al., *The epidemiology of revision total hip arthroplasty in the United States.* J Bone Joint Surg Am, 2009. 91(1): p. 128-33.**
7. **Wedemeyer, C., et al., *Particle-induced osteolysis in three-dimensional micro-computed tomography.* Calcif Tissue Int, 2007. 81(5): p. 394-402.**
8. **Caetano-Lopes, J., H. Canhao, and J.E. Fonseca, *Osteoblasts and bone formation.* Acta Reumatol Port, 2007. 32(2): p. 103-10.**
9. **al., F.e., *Kelley's Textbook of Rheumatology Volume I*. Vol. 9. 2012. 61-66.**
10. **Purdue, P.E., et al., *The central role of wear debris in periprosthetic osteolysis.* HSS J, 2006. 2(2): p. 102-13.**
11. **King, A.E., et al., *Nucleoside transporters: from scavengers to novel therapeutic targets.* Trends Pharmacol Sci, 2006. 27(8): p. 416-25.**
12. **Fredholm, B.B., et al., *International Union of Basic and Clinical Pharmacology. LXXXI. Nomenclature and classification of adenosine receptors--an update.* Pharmacol Rev, 2011. 63(1): p. 1-34.**
13. **Fredholm, B.B., et al., *International Union of Pharmacology. XXV. Nomenclature and classification of adenosine receptors.* Pharmacol Rev, 2001. 53(4): p. 527-52.**
14. **Mediero, A., et al., *Adenosine A(2A) receptor ligation inhibits osteoclast formation.* Am J Pathol, 2012. 180(2): p. 775-86.**
15. **Golub, E.E., et al., *The role of alkaline phosphatase in cartilage mineralization.* Bone Miner, 1992. 17(2): p. 273-8.**
16. **Termine, J.D., et al., *Osteonectin, a bone-specific protein linking mineral to collagen.* Cell, 1981. 26(1 Pt 1): p. 99-105.**
17. **Delany, A.M. and K.D. Hankenson, *Thrombospondin-2 and SPARC/osteonectin are critical regulators of bone remodeling.* J Cell Commun Signal, 2009. 3(3-4): p. 227-38.**

18. Niyibizi, C. and D.R. Eyre, *Structural characteristics of cross-linking sites in type V collagen of bone. Chain specificities and heterotypic links to type I collagen.* Eur J Biochem, 1994. 224(3): p. 943-50.
19. Hauschka, P.V., et al., *Osteocalcin and matrix Gla protein: vitamin K-dependent proteins in bone.* Physiol Rev, 1989. 69(3): p. 990-1047.
20. Lam, J., et al., *TNF-alpha induces osteoclastogenesis by direct stimulation of macrophages exposed to permissive levels of RANK ligand.* J Clin Invest, 2000. 106(12): p. 1481-8.
21. Ducy, P., et al., *Increased bone formation in osteocalcin-deficient mice.* Nature, 1996. 382(6590): p. 448-52.
22. Sodek, J., B. Ganss, and M.D. McKee, *Osteopontin.* Crit Rev Oral Biol Med, 2000. 11(3): p. 279-303.
23. Wada, T., et al., *RANKL-RANK signaling in osteoclastogenesis and bone disease.* Trends Mol Med, 2006. 12(1): p. 17-25.
24. Takeichi, M. and T.S. Okada, *Roles of magnesium and calcium ions in cell-to-substrate adhesion.* Exp Cell Res, 1972. 74(1): p. 51-60.
25. McInnes, I.B. and G. Schett, *Cytokines in the pathogenesis of rheumatoid arthritis.* Nat Rev Immunol, 2007. 7(6): p. 429-42.
26. Sato, K., et al., *Th17 functions as an osteoclastogenic helper T cell subset that links T cell activation and bone destruction.* J Exp Med, 2006. 203(12): p. 2673-82.
27. Zwerina, J., et al., *TNF-induced structural joint damage is mediated by IL-1.* Proc Natl Acad Sci U S A, 2007. 104(28): p. 11742-7.
28. McClung, M.R., et al., *Denosumab in postmenopausal women with low bone mineral density.* N Engl J Med, 2006. 354(8): p. 821-31.
29. Matsuo, K. and N. Irie, *Osteoclast-osteoblast communication.* Arch Biochem Biophys, 2008. 473(2): p. 201-9.
30. Zhao, C., et al., *Bidirectional ephrinB2-EphB4 signaling controls bone homeostasis.* Cell Metab, 2006. 4(2): p. 111-21.
31. Hartmann, C., *Transcriptional networks controlling skeletal development.* Curr Opin Genet Dev, 2009. 19(5): p. 437-43.
32. Lorenzo, J., M. Horowitz, and Y. Choi, *Osteoimmunology: interactions of the bone and immune system.* Endocr Rev, 2008. 29(4): p. 403-40.